Members Only
R&D REPORT
NO. 116

Optimising in-container mixing conditions to enhance heat transfer to thermally processed foods

2000

Campden BRI

Campden BRI

Chipping Campden
Gloucestershire
GL55 6LD, UK

Tel: +44 (0)1386 842000
Fax: +44 (0)1386 842100
www.campden.co.uk

Members Only
R&D Report No. 116

Optimising in-container mixing conditions to enhance heat transfer to thermally processed foods

S Emond and G Tucker

2000

SUMMARY

Rotary processing can significantly improve the heating rate in a food, giving reduced processing times, increased product throughput, reduced energy costs and improved product quality. Whilst a rotational process can achieve all of these things, very often the speed chosen is not optimal and is established by historical methods rather than by matching the speed to the product characteristics.

A numerical simulation model was used to identify the shear rates achieved in a rotating container and these values were used to rheologically characterise a tomato sauce product. Typical shear rates within the food ranged from 0 to $6s^{-1}$ at rotational speeds up to 40 rpm. Simulants were identified that had similar flow characteristics at ambient temperature (25 °C) to the product at elevated temperatures.

Jars containing the simulants were rotated at ambient temperature in a pilot scale retort under end over end conditions at different rotation speeds. Flow visualisation trials determined the time required to incorporate a dye into the solutions at different speeds and a process with modified rotational speeds was designed to match the rheology of the product.

The rotational process was validated by both pilot and industrial scale trials, testing the existing "standard" process against the optimised rotational process. Comparing the time taken for products to achieve a set pasteurisation value, savings in processing time of between 13% and 30% were achieved by matching the optimal mixing speed to the flow characteristics of the product.

In general, it was noted that the rotational speeds currently employed by many processors are below those required to optimise the benefits of rotary processing. The speeds used in these trials are achievable with current rotary equipment; however, a balance should be sought between achieving the process time savings and the extra cost incurred by further wear and tear on the equipment due to higher stresses incurred at higher rotational speeds.

TABLE OF CONTENTS

1.	INTRODUCTION AND BACKGROUND	1
2.	METHODS	5
2.1	Numerical solution of the flow	5
2.2	Rheological classification	6
2.3	Flow visualisation of simulants	6
2.4	Thermal processing	7
3	RESULTS	10
3.1	Numerical simulation of the flow	10
3.2	Rheological classification	10
3.3	Flow visualisation of simulants	13
3.4	Thermal processing	15
4	DISCUSSION	20
5	CONCLUSIONS	22

REFERENCES

Appendix 1: Rheological data for tomato sauce at elevated temperatures

Appendix 2: Rheological data for Colflo 67 at ambient temperature

Appendix 3: Flow visualisation results

Appendix 4: Predicted processing profiles

Appendix 5: Heating profiles for factory trials

1. INTRODUCTION AND BACKGROUND

The present food industry approach to the selection of rotary processing conditions for products is based on experience and measurements from limited numbers of samples. Most rotation rates are based on existing steriliser operating values, although these can correspond to different products, processes and containers. These are likely to be far removed from the optimal conditions. Variations in factors such as container shape, product viscosity and rotation speed can have a great effect on the internal mixing within a container and therefore on the rate of heat penetration into the product.

Rotation for batch thermal processing falls into two categories: firstly, end-over-end (EoE) processing, where a retort crate rotates around a central horizontal axis and the containers sit vertically; and secondly axial rotation, where cans are rotated in the horizontal plane. Clifcorn et al (1950) looked at the advantages of agitating cans during EoE and axial rotation methods. Using high rotation rates and high temperatures gave an overall improvement in product quality, particularly for viscous and heat sensitive products. EoE methods gave better results at lower rotation speeds (less than 120rpm); above this the results were equal.

Several studies have identified that mixing via the headspace bubble can have a significant effect on the heat transfer within the product. Conley et al (1951) showed that, as the speed of rotation increased beyond the optimal centrifugal force, the movement in the product reduced; this effect was dependent upon the radius of rotation. Parchomchuk (1977) and Naveh and Kopelmann (1980) looked at this effect for both EoE and circular agitating product. Rotation speed, viscosity and headspace were investigated and it was found that maximum heat transfer was achieved during EoE rotation with large headspaces at speeds from 40 to 80 rpm. Berry et al (1979) looked at the effect of an increasing headspace during the processing of cream style corn, where gases are released from the product, thus increasing the headspace. This increase in headspace was found to dramatically increase the sterilisation value achieved. Decreasing the headspace decreased the rate of heat penetration and therefore the sterilisation value F_0. For example, at 10rpm the heating factor, f_h, was increased from 10 minutes to 50

minutes with a decrease in headspace from 10/32" to 4/32". In all cases, the headspace bubble flow pattern was given as the reason for the difference in heat transfer between the cans. Theoretically, as the size of a bubble increases so its relative velocity increases, thus improving the mixing. However, beyond a certain point, due to an increase in bubble deformation, the increased bubble size will probably increase drag on the walls and therefore decrease the mixing effects of the bubble. Secondly, an increase in heat penetration rates may be offset by viscous forces within the can which oppose product movement at higher oscillating speeds.

Studies by Javier et al (1985) and Ramaswamy et al (1993) looked further into the effect of viscosity, mode of rotation, can size and rotation speed on the heating factor (f_h) of products. In both studies, the results showed an increase in f_h with an increase in viscosity of the product and a decrease in f_h with increasing rotation speed. In all cases, higher heating rates were achieved in EoE than axially rotating or reel and spiral simulation cans. A further finding was that in EoE and reel and spiral simulation the f_h value decreased with increasing rotation speed; however, in axial rotation there was a zone where an increase in rotation speed led to an increase in f_h value. After this zone, the heating rates increased with increasing rotation speed. In axially rotating cans, bubble movement had two effects: increasing the rotation disrupted the streamlines, therefore promoting convective transfer to the centre, but this also meant that the bubble moved to the centre of the pack, thus slowing down the heating rate. The movement of the bubble to the centre of the can did not occur in the EoE cans; this was thought to be due to the strong end effect of the packaging as it rotates.

Britt et al (1994) looked at the radial position during rotation and processing conditions on the uniformity of product heating. A 1% (w/v) bentonite solution was filled into 76.2 x 115.9mm cans with a 5% headspace and closed without vacuum. Different positions were looked at within a retort basket, plus rotational speeds of 0, 10 and 20 rpm. It was found that whilst rotation resulted in higher F_0 values, this was not consistent through the product load. The lowest F_0 value varied throughout the load, with no one position being identified as the worst place within the basket; this agreed with the findings of Anantheswaran and Rao (1985). In contrast Knap and Durance (1998) investigated the

effect of radial position on f_h in a potato in water product. They concluded that radial position did influence heating rates in both the liquid and particle phase with f_h decreasing as the distance from the axis of rotation increased. A possible explanation could be that moving the can away from the central axis improved the heat transfer coefficient, because the centripetal acceleration increased with increasing radial position, giving rise to greater relative bubble velocity.

Stoforos and Merson (1991,1992) studied the use of aluminium and Teflon particles to determine the uniformity of heating under axial can rotation with different viscosity liquids. Liquid crystals were used as temperature sensors for measuring the particle surface temperatures. In general, it was found that liquid-particle film heat transfer coefficients increased with increasing rotational speed and increasing fluid viscosity; however, the overall heat transfer coefficient (heating medium/container wall/internal liquid) decreased with increasing fluid viscosity but increased with increasing rotational speed. Knap and Durance (1998) investigated the difference in sterilisation values between particles moving freely in a low viscosity liquid solution and a particle suspended on a mock thermocouple. In all cases, a higher sterilisation value was achieved on the suspended particle; this was thought to be due to the relative velocity between the fluid and the particle. Where a particle is free to move and the solid and liquid phase have similar densities, there will be less drag forces on these particles than on the suspended particle, so resulting in a lower sterilisation value in the freely moving particles.

Sablani and Ramaswamy (1995) looked at the fluid-to-particle heat transfer coefficients in cans during EoE processing. Using water and oil as the liquid phases and polypropylene spheres as the particles, heat penetration trials were carried out at three retort temperatures and four rotation speeds. The results showed that rotation speeds had a greater influence than temperature on the fluid to particle heat transfer coefficient. On average, the fluid-to-particle heat transfer coefficient increased four fold as the rotational speed increased from 0 to 20 rpm, whilst an increase in retort temperature from 110 °C to 130 °C resulted in only a 10% increase. It was also found that an increase in rotation speed resulted in an increase in the overall heat transfer coefficient, as did an increase in retort temperature. For all of these effects it was concluded that increases in heat transfer coefficient due to

rotation speed could be attributed to the increased turbulence within the container. Increasing the retort temperature probably led to a reduction of the viscosity of the product, so increasing the heat transfer coefficient

A wide range of work has been carried out in this area; however, in all cases although viscosity has been identified as an area of importance, the trials have been on single viscosities only and have not taken into account the changes that will occur in the product as it is heated. Although it is known that the headspace bubble aids mixing, and the optimum mixing will be dependent on product viscosity, the rotation speeds necessary for maximum mixing will vary as the product viscosity changes.

To quantify this, initial trials were carried out looking at commercially available sauces at a range of temperatures. Once the rheological characterisation of each product had been identified, a range of transparent and semi-transparent solutions were assessed to try and match the viscosities of the products at different temperatures with simulants to be used at ambient temperature. Comparing transparent simulants with commercially available sauces at different temperatures would therefore allow trials to be carried out at ambient temperature using simulants of the same viscosity.

The objectives of this study were to:

(1) understand the mixing patterns that occur within an end-over-end rotating container with varying rotation speeds and viscosities
(2) match the rheological characteristics of commercially available products at different temperatures with simulants to observe the mixing patterns at different viscosities
(3) calculate the shear rates that occur within a rotating container using computational fluid dynamics modelling
(4) optimise the process for the commercial product using the visualisation, rheological analysis and modelling
(5) verify the process by carrying out heat penetration trials on the product using the new optimised process.

2. METHODS

2.1 Numerical Simulation of the Flow

Numerical simulation of the flow inside a rotating container was carried out in order to establish the shear rates in the containers to ensure that further rheological models were applied in the correct working range. With most in-pack processed foods exhibiting non-Newtonian rheology, this step was essential in order to define the shear rate range for measuring rheological properties.

To achieve this, the flow of liquid inside a can, with a 10% gas headspace, rotating about its axis was numerically simulated using the CFX 4.1 Computational Fluid Dynamics software (AEA Technology). Newtonian and generalised non-Newtonian fluids were considered and the results validated in two ways.

Firstly, experimental observations of the headspace bubble location and shape were compared with those predicted numerically. The experiments were carried out for a range of rotational speeds (10–50 r.p.m.) and for several fluids.

Secondly, measurements of wall shear stress were made, using hot-film probes and constant temperature anemometry, on the curved and flat end-walls of the can as it rotated. The numerically predicted wall shear stresses were then compared with the measurements, again for different fluids, a range of rotational speeds and for on- and off-axis rotation.

The numerical solutions, once validated, allow details of the velocity and shear rate fields to be examined. The working range for the shear rates was found to be from 0 to $6s^{-1}$.

2.2 Rheological Classification

Rheological tests, using a controlled shear stress rheometer (Carrimed, UK), were undertaken with a double concentric cylinder cell with wide gap to accommodate any small particles in a product. The cell was surrounded by a heating coil on the inner and outer cylindrical surfaces in order to strictly control the temperatures in the test cell. Rheological tests for simulants (products containing no particulate matter) were tested using a Contraves Rheomat-30 (Contraves AG, Zurich).

2.2.1 Product rheology at elevated temperatures

A tomato based sauce containing small vegetable particles and a modified maize starch thickener was tested at a range of temperatures in the double concentric cylinder cell. Over the shear rates of interest, 0 to 6 s^{-1}, the Careau model was applied. However, the shear rate region between 0.06 s^{-1} and 6s^{-1} included most of the flow inside the rotating can (predicted from the numerical solutions) and so this power law region was used to compare the product rheology to that of the simulants.

2.2.2 Simulant rheology under ambient conditions

Several transparent and opaque solutions were tested at ambient conditions (25 °C) using either the Carrimed cone and plate or the Contraves concentric cylinder rheometers. Different concentrations of simulant solution were tested to find solutions matching the rheological characteristics of the tomato sauce at elevated temperatures. Based on this data, the concentrations for the flow visualisation studies were identified.

2.3 Flow Visualisation of Simulants

A glass jar of dimensions 152mm height, 64mm neck width, and 76mm body width was filled to 490g with a 6.29% w/w Colflo67 starch solution (National Starch & Chemical Ltd., Manchester) plus 10g 6.29% w/w Colfo67 starch solution mixed with blue food dye

(Pointing Ltd., Prudhoe, Northumberland NE42 6NJ), giving a headspace of 10 mm at ambient temperature (25 °C).

The jar was placed in a pilot scale Stock Rotomat PRU 900 (Hermann Stock Maschinenfabrik GmbH, Neumunster, Germany) on the central axis of rotation. The jar was rotated under end-over-end conditions initially at 15rpm. The movement of the jar was recorded using a JVC digital video camera over a three minute period to assess the homogeneity of incorporation of the dye into the starch solution. The images were captured at one minute intervals using JLIP video capture software, version 1.0, in order to assess the mixing. The trial was then repeated at 20, 25 and 30 rpm and at intermediate speeds to find the optimum mixing speed.

The images were compared to give process rotation speeds which would give optimal mixing in the product.

The trial was then repeated with starch solutions of 5.97, 5.73, 5.58 and 5.48 % under the same conditions. The images for each of these solutions were assessed, giving optimum process rotation conditions for the product as its viscosity changed with temperature throughout a process.

2.4 Thermal Processing

2.4.1 Pilot scale trials

The tomato sauce was filled into jars (as described in 2.3) to a fill weight of 500g giving an 8mm headspace. The jars were placed on the central axis of rotation in a pilot scale Stock Rotomat PRU 900. The jars were then processed using the standard processing conditions for the product (full water immersion, 100 °C at 15rpm for 30 minutes). The trial was repeated with jars filled to 500g and then subjected to the modified (optimised) rotational process based upon the results of the visualisation trials. The time and temperature data from each of the trials were recorded with an Ellab CMC92 datalogger

(Ellab UK Ltd., Kings Lynn). When the product reached the test temperature of the rheological analysis, the rotation speed was modified to match the optimal mixing conditions found from the visualisation trials.

Minor changes in retort processing conditions between runs (sample initial temperature, sterilisation temperature and retort come up time) were removed from the analysis by standardising the sterilisation times and conditions for each of the trials using the CCFRA CTemp model (Tucker *et al*, 1996). Heating factors (f_h values) were calculated from the time and temperature data and used as product heating rates in the CTemp model. The model was used to predict the time to achieve the target P_u value (reference temperature 93.3°C, z 8.3C°) of 10 minutes at the end of heating for both the standard and optimised trials.

2.4.2 Factory trials

The tomato sauce was prepared as a standard batch and filled into the jars to a maximum fill weight of 330g. Standard product jars were used of dimensions 132mm height, 64mm neck width and 76mm body width (headspace 8mm). Heat penetration trials were carried out at the factory using Ellab A10 (85mm) needle probes (Ellab UK Ltd. Kings Lynn) with 20mm spacers, placed through the lid of the jar.

The products were processed in a four basket Stock Rotomat using a full water immersion process at a process temperature of 100°C, with a rotation rate of 15 rpm. The product was held at process temperature for 30 minutes according to the production scheduled process. Results were recorded at 30 second intervals using an Ellab CMC 821 datalogger connected to a computer using Ellab PCLink92 software. This gave the data against which the processes with modified rpm were compared.

A second trial was carried out using the same procedures; however, once the product reached the temperatures used in the rheological analysis, the rotation rate was manually changed to the speeds identified in the visualisation trials. A third trial was carried out repeating the manually interrupted conditions, but programming the controller to

automatically increase the rotation rate based upon the times to achieve set temperatures found in the second trial.

The results for each trial were analysed using the CTemp programme to assure consistency between conditions and calculate the heating factors (f_h) for each replicate. The results were compared by using the same retort profile and initial product temperature to establish if there had been any reduction in the required process times.

Observation of differences in product quality were carried out immediately after the trials and after 8 weeks' storage at ambient temperature. The key aim was to avoid separation. In addition, a taste panel was set up to blind taste the three products.

3. RESULTS

3.1 Numerical Simulation of the Flow

The results of the numerical simulations showed the shear rates in the containers to be between 0 s^{-1} and 6s^{-1}. These values were critical and allowed the rheological analysis of the simulants and tomato sauce to be assessed in the correct region for shear rate.

3.2 Rheological Classification

3.2.1 Product rheology at elevated temperatures

Appendix 1 contains the spreadsheets of rheological data modelled using the power law. Table 1 gives a summary of the consistency coefficients (k) and flow behaviour indices (n) and apparent viscosities at a shear rate of 10s^{-1}. Figure 1 shows the change in apparent viscosity with shear rate for temperatures between 40 and 80 °C.

Table 1: Product characteristics for tomato sauce at elevated temperatures

Product Temperature (°C)	k (Pa.s^n)	n	Apparent viscosity at shear rate 10s^{-1} (Pa.s)
40	25.56	0.27	4.76
50	21.94	0.28	4.21
60	18.46	0.32	3.84
70	16.47	0.34	3.57
80	14.62	0.37	3.44

Figure 1: Apparent viscosity of tomato sauce at elevated temperatures at a range of shear rates

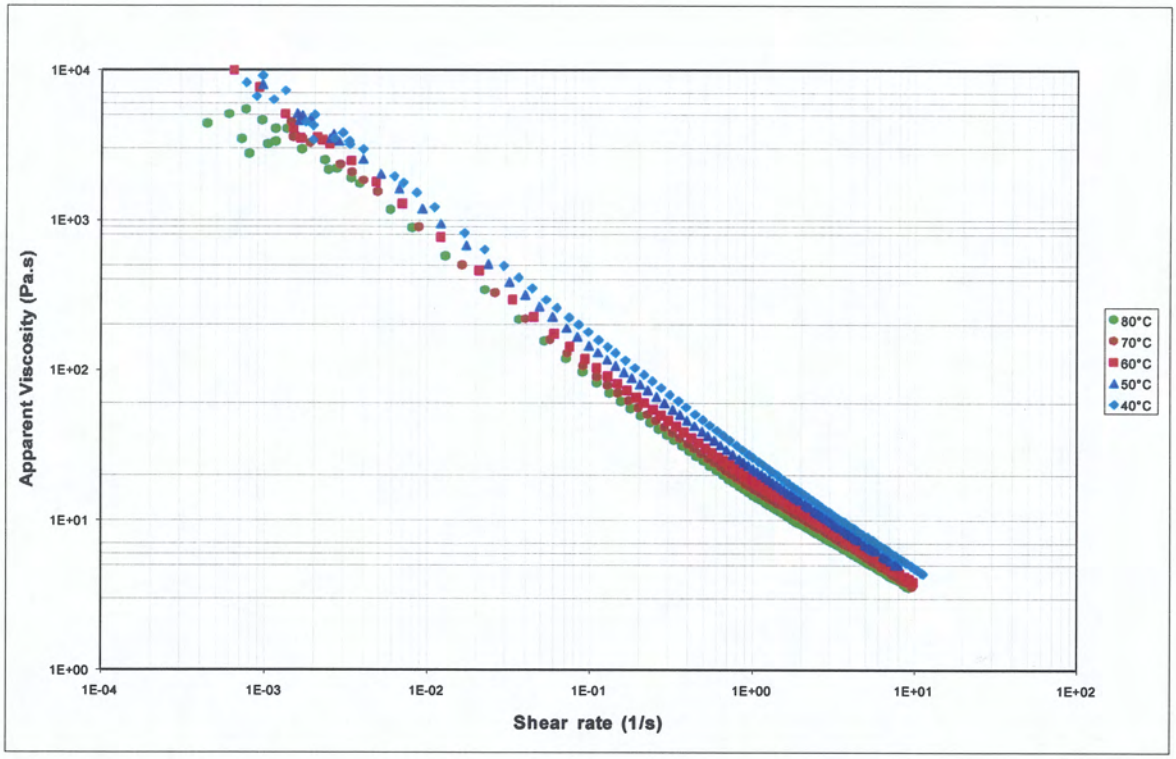

3.2.2 Rheology of simulants at ambient temperatures

Appendix 2 shows the rheological data modelled using the power law. Table 2 shows the rheological results for solutions of Colflo 67 at 25°C. Figure 2 shows the power law model applied to Colflo 67 solutions at 25°C. From the rheological data the equivalent concentrations of Colflo 67 to match the tomato sauce at temperatures of 40, 50, 60, 70 and 80°C were estimated. Table 2 gives a summary of the consistency coefficients (k), flow behaviour indices (n) and apparent viscosities at a shear rate of $10s^{-1}$. Table 3 shows the concentration of Colflo 67 solution that matches the rheological behaviour of tomato sauce at the elevated temperatures.

Table 2: Rheological results for Colflo 67 simulant solutions

Colflo 67 solution % (w/w)	k ($Pa.s^n$)	n	Apparent viscosity at shear rate $10s^{-1}$ (Pa.s)
5.5	19.74	0.24	3.44
6.0	25.27	0.23	4.34
6.5	28.44	0.27	5.24
7.0	42.72	0.24	7.51

Figure 2: Apparent viscosity of Colflo 67 solutions at ambient temperature for a range of shear rates

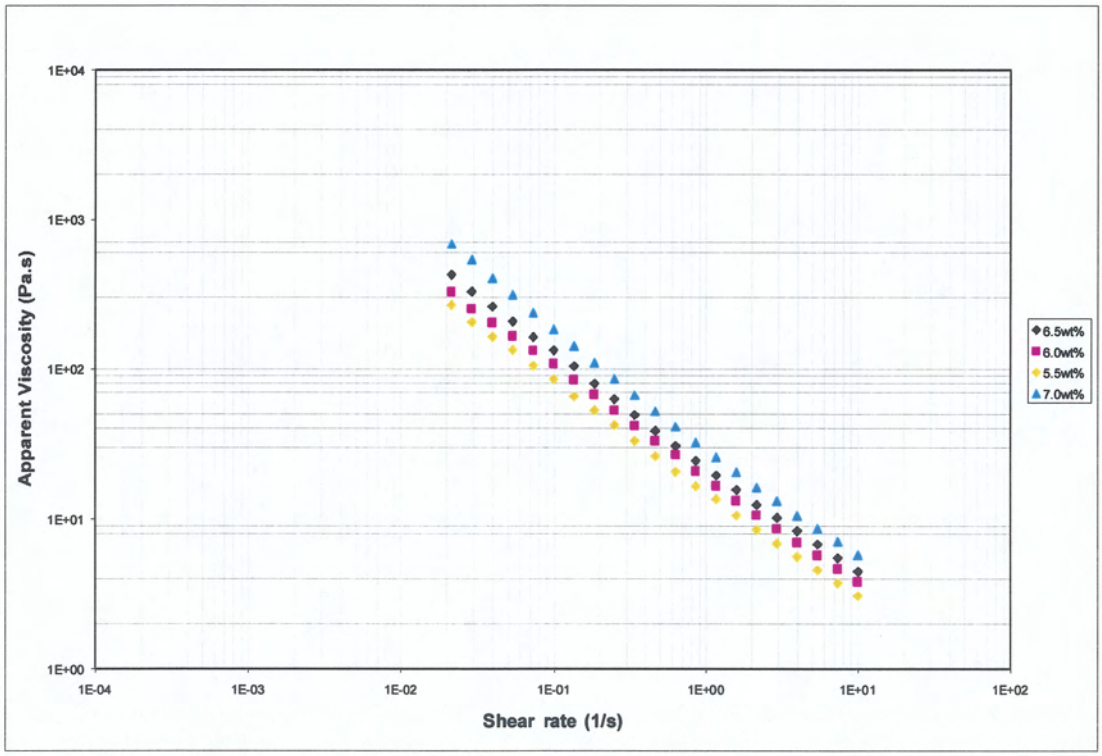

Table 3: Concentration of Colflo 67 solutions to simulate the power law values for tomato sauce for a range of temperatures

Product temperature (°C)	Colflo 67 solution % (w/w)
40	6.29
50	5.97
60	5.73
70	5.58
80	5.48

3.3 Flow Visualisation of Simulants

Figure 3 shows the results taken at one minute intervals after incorporation of dye into the starch solutions. Appendix 3 shows the results of all of the flow visualisation trials for the Colflo 67 solutions at different concentrations. From the results of the visualisation trials (degree of incorporation of blue dye into the solution) an optimised rotation profile was established. Interpretation of the blue coloration was used, but this was complicated by the position of the headspace bubble. Some still photos taken from the video appeared less mixed than when continuously viewed, for example at 22 and 25 rpm. At 22 rpm and 3 minutes, the still photo includes the headspace bubble elongated at the right hand jar side. Table 4 shows the optimised rotation profile achieved for product as it reaches the temperatures corresponding to the Colfo 67 at different concentrations and the quantity of blue dye incorporated into these solutions.

Figure 3: Blue dye incorporation into 6.29% Colflo 67 starch solution when mixing at different rotation speeds

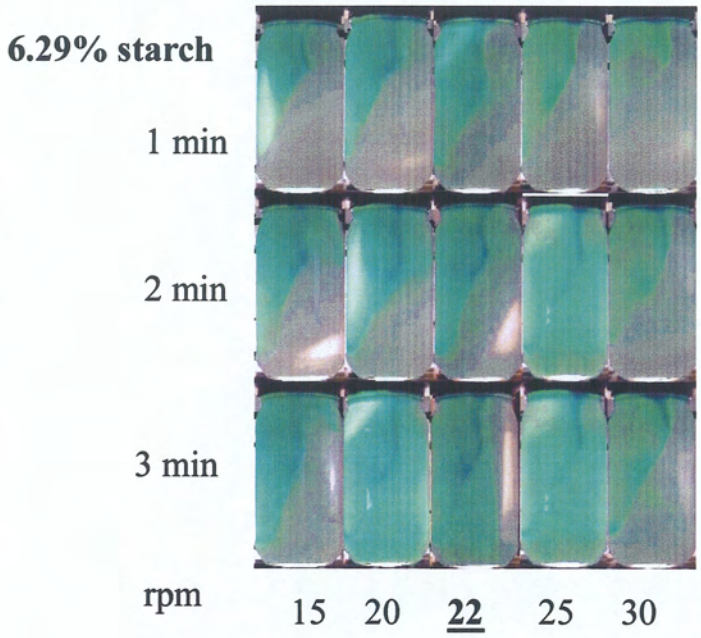

Table 4: Optimised rotation speeds for mixing in the product at different temperatures.

Product temperature (°C)	Rotation speed (rpm)
20	15
40	22
50	22
60	27
70	27
80	30

3.4 Thermal processing

3.4.1 Pilot scale trials

The results of the pilot scale trials for the standard rotation conditions can be seen in table 5 and for the optimised rotation in table 6. The heating factor was calculated and the end of heating pasteurisation value together with the time to P 10 were predicted for consistent retort and product conditions. The products processed under optimised conditions showed broken heating characteristics due to the changes in the heating rate that occured as the rotation speed changed (Table 6). Appendix 4 shows the process as calculated on the CTemp software. Figure 4 shows a comparison of the heating profiles for the product processed under standard conditions against the product processed under optimised conditions, and Table 7 shows a summary of data for the time taken to reach P 10 for standard and optimised processes. The reduction in process times achieved with the optimised process was between 12% and 24%. However, it is likely that this will be greater with industrial processes that do not contain such a large come-up contribution.

Table 5: Heating factors for jars of tomato sauce processed under standard retort conditions

Product Replicate	f_h (mins)	End of heating P value prediction (after 25 minutes hold)	Time to P 10 (minutes)
1	9.5	52.6	16.5
2	11.7	59.6	16.0
3	13.5	43.7	18.5

Table 6: Heating factors for jars of tomato sauce processed under optimised retort conditions

Product replicate	f_{h1} (mins)	f_{h2} (mins)	X_{bh} (mins)	End of heating P value prediction after 25 minute hold	Time to P 10 (minutes)
1	11.2	6.1	4.5	76.2	14.0
2	12.9	6.5	3.3	76.6	13.5
3	74.8	5.1	6.3	75.7	14.0

Figure 4: Heating profiles of standard and optimised processes for jars of tomato sauce

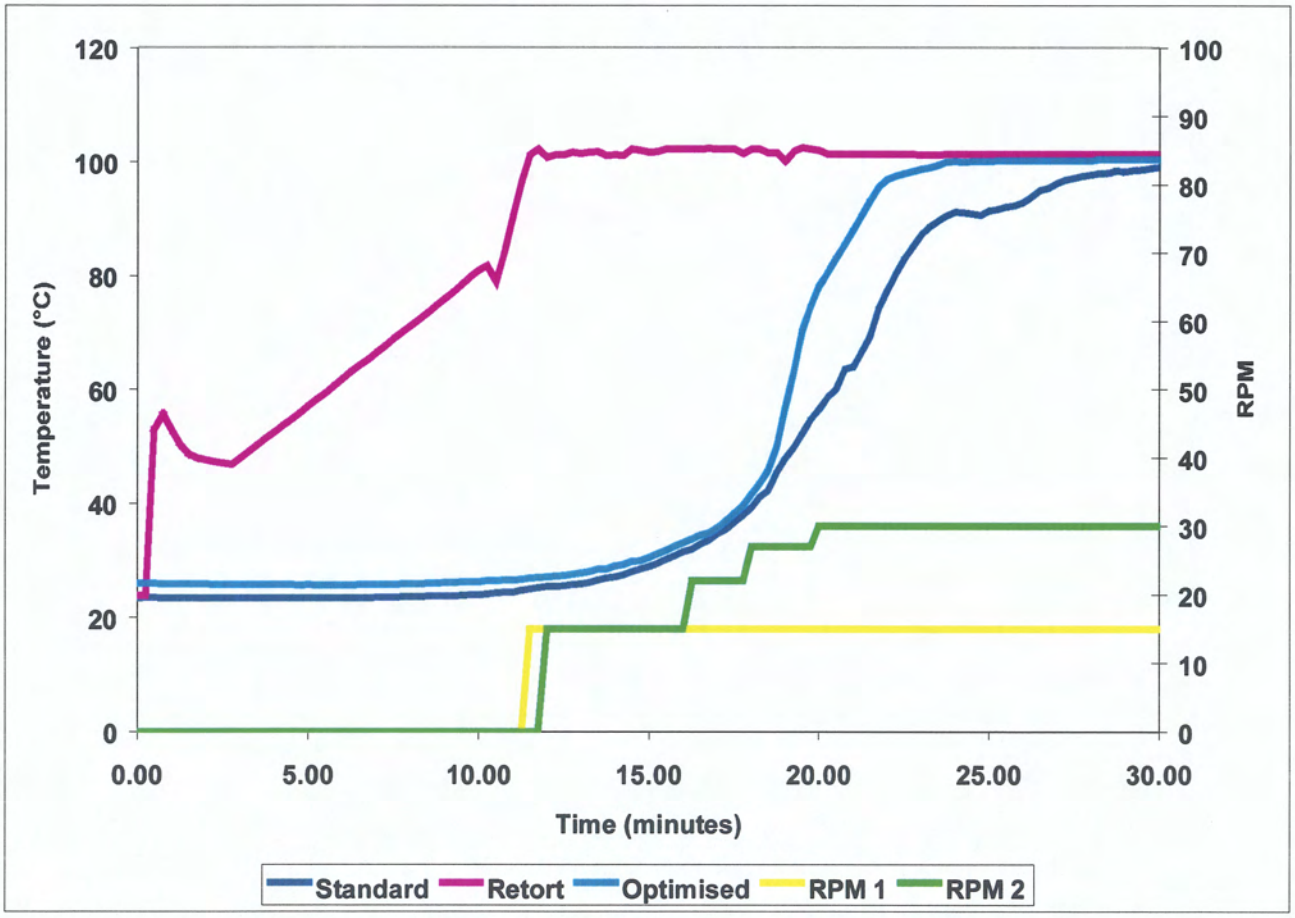

Table 7: Calculated time taken for tomato sauce to reach P 10 for standard and optimised processes.

Replicate	Time to P 10 (Reference temperature 93.3°C, z 8.3C°) (minutes)		
	Standard process	Optimised process	% Reduction
1	16.0	14.0	12.5
2	16.0	13.5	15.6
3	18.5	14.0	24.3

3.4.2 Factory trials

The results of the factory trials for the standard retort conditions can be seen in table 8 and for the optimised rotation in table 9. The heating factor, the end of heating pasteurisation value and time to P 10 using standard conditions have been calculated. Large f_h values at the start of the process represented the period when the retort rpm was zero as the water filled the retort. Small differences in the time to fill the retort resulted in large differences between the f_h values in tables 8 and 9. Appendix 4 shows the process as calculated by the CTemp software. Appendix 5 gives the time-temperature profiles from each of the trials. Figure 4 shows a comparison of the heating profiles for the product processed under standard conditions against the product processed under optimised conditions. This showed that the optimised processes delivered a faster rate of heat penetration than the standard processes. Table 10 shows a summary of data for the time taken for tomato sauce to reach P 10 for standard and optimised processes. Table 11 summarises the results of the informal sensory analysis after processing and after storage which indicate no obvious differences between the standard and optimized (manually timed) processes.

Table 8: Product heating rates for tomato sauce processed under standard conditions

Product replicate	f_{h1} (min)	f_{h2} (min)	f_{h3} (min)	End of heating P (20 minutes)	Time to P10 (min:sec)
1	92.6	5.6	6.7	33.4	13:30
2	145.3	6.7	7.4	24.5	15:00
3	65.5	5.8	8.6	24.9	14:30

Table 9: Product heating rates for tomato sauce processed under optimised conditions

Product replicate	f_{h1} (min)	f_{h2} (min)	f_{h3} (min)	End of heating P	Time to P10 (min:sec)
Manual 1	39.9	4.2	6.8	47.6	11:00
Manual 2	155.2	4.0	6.1	54.5	10:00
Manual 3	78.9	4.2	6.1	49.4	11:00
Automatic 1	41.3	2.6	8.2	39.2	11:30
Automatic 2	38.7	2.7	7.5	45.1	11:30
Automatic 3	63.3	3.7	8.0	42.9	11:30

Figure 5: Heating profiles for manual, timed and standard process

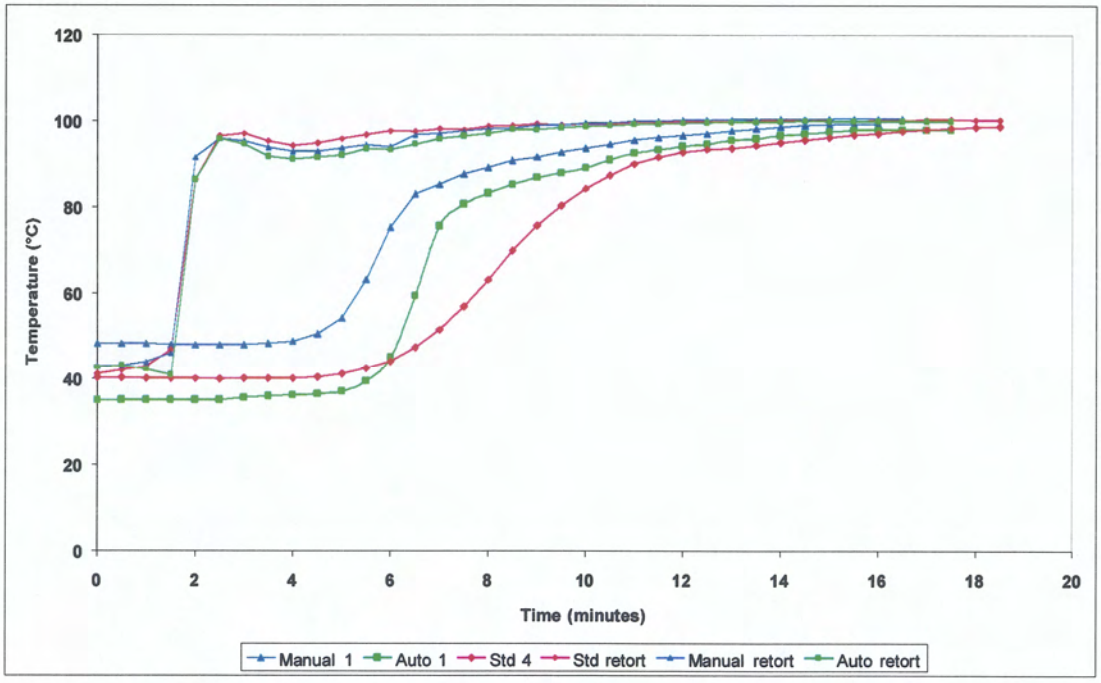

Table 10: Summary of the time taken at constant retort temperature for tomato sauce to achieve P 10

Replicate	Time to P10, reference temperature 93.3°C, z 8.3C°C (min:sec)		
	Standard	Manually timed	Automatically timed
1	13:30	11:00	11:30
2	15:00	10:00	11:30
3	14:30	11:00	11:30

Table 11: Informal taste panel results after processing and after storage

Process	After processing	After storage
Standard	As expected	As expected
Manually timed	Similar colour to standard, possibly a little paler. No visible separation	Similar colour to standard product. No visible separation. No perceptible difference in flavour attributes
Automatically timed	Similar colour to manually timed, no visible separation	Similar colour to standard. No visible separation. No perceptible difference in flavour attributes.

4. DISCUSSION

In order to ensure that the rheological classification of the sauces was being carried out in the correct shear rate range, it was necessary to establish the shear rate in a rotating container. These data were not available in the scientific literature because there are no reliable methods for measuring shear rate distribution. The numerical simulations showed that the range within a container was low, between 0 s^{-1} and 10 s^{-1}. A low range was expected for end-over-end rotation but could not be assured until the simulations confirmed the absolute values. From this information, the rheological characteristics of both the tomato sauce and the simulants were calculated within the correct shear rate range.

The rheological data for the tomato sauce showed that the apparent viscosity reduced as its temperature increased, the typical response of most materials. To simulate this reduction in viscosity, concentrations of Colflo 67 were reduced from 6.29 to 5.48 wt%. This allowed the changing viscosity as a function of temperature to be simulated with a range of solutions at ambient temperature. This was a critical step that allowed flow visualisation studies to be conducted.

The flow visualisation trials never attained the perfect mixing pattern of the bubble moving through the centre of the jar as the jar turned end-over-end. As the CFD simulations become more advanced it should be possible to predict the combination of product, package and process condition that can result in the bubble moving through the jar centre line.

From the data it was seen that as the rotation speed increased, the incorporation of dye into the solution improved, indicating that most current processing speeds were too low. However, rather than recommending that rotation speeds are automatically increased to the maximum that can be practically achieved, the situation is more complex. For example, figure 1 shows the mixing in the thickest solution (6.29% starch, equivalent to tomato sauce at 40°C) at 30 rpm to be very similar to that achieved at 15 rpm. This was thought to be because at 15 rpm the headspace bubble, which was acting as the agitator in

the jar, had time to deform and moved slowly around the outside of the jar without disrupting the central area of the product. At 30 rpm, the speed of rotation was too high to allow the bubble time to deform and to move through the product because of drag on the surfaces. The mixing for 6.29% starch was seen to be optimal at 22 rpm. In general, as the product became less viscous (as it heated up) the speed of mixing needed to be increased, showing less drag as the bubble moved through the product, in order to improve mixing in the jar.

The pilot scale trials verified the improved mixing in a heated system. By calculating the heating factors for the products under both standard and optimised mixing conditions and using the information in a standard heating profile, the direct comparison of time taken to reach a set pasteurisation value showed that the optimised profile improved the heat penetration into this product by between 12.5% and 26.5%.

The factory trials also verified the improvements in in-container mixing and these trials took into account product make-up differences, thus standardising variations that occur in manufacture. The results showed a saving in processing time of between 15 and 30%. Eight weeks after the processing, the products were tested by informal taste panel. The panel concluded that by changing the process the product had not suffered any detrimental effects. The sauce had not separated (a key attribute of this product) and was acceptable when processed under standard and optimised conditions.

5. CONCLUSIONS

The high rotation speeds used in these trials can be achieved with current rotary equipment; however, a balance must be reached between process time savings and additional costs incurred by further wear and tear on the equipment. In addition, it is necessary to prove that the increased centrifugal forces do not act to reduce the heat transfer efficiency at the centre of a retort crate. This has implications for all types of heating media but it is the raining water and steam/air mixtures that may be the most affected.

Matching the rheological characteristics of a heating product to a simulant at ambient temperature was a successful method that enabled the mixing in the container to be clearly seen at ambient temperatures via dye incorporation. To enable mixing to be optimised for other products, a large amount of background work on their rheological characterisation is necessary. The future aims for this area will be to combine the CFD models being developed with known rheological data for products in order to predict the optimal processing conditions. This should reduce the need for identification of suitable simulants which would then be observed by flow visualisation. This type of numerical model will enable decisions to be made regarding optimal processing conditions that will reduce processing times whilst maintaining product quality and safety.

References

Anantheswaran, R.C. and Rao, M.A. (1985). Heat transfer to model Newtonian liquid foods in cans during end over end rotation. Journal of Food Engineering 4 (1), 1-19.

Berry, M.R., Savage, R.A. and Pflug I.J. (1979). Heating characteristics of cream style corn processed in a steritort: effects of headspace, reel speed and consistency. Journal of Food Science 44, 831-835.

Britt, I.J., Paulson, A.T., Stark, R. and Tung, M.A. (1994). Heat transfer in liquid filled containers during end over end rotation. In: Developments in Food Engineering. Ed. Yano, T., Matsuno, R. and Nakamura, K. 716-718.

Clifcorn, L.E., Peterson, G.T., Boyd, J.M. and O'Neil, J.H. (1950). A new principle for agitating in processing of canned foods. Food Technology 4, 450-460.

Conley, W., Kaap, L. and Schuhmann, L. (1951). The application of 'end-over-end' agitation to the heating and cooling of canned food products. Food Technology 5, 457-460.

Holdsworth, S.D., (1997). Thermal Processing of Packaged Foods. Blackie Academic and Professional, London, UK.

Javier, R.A., Naveh, D., Perlstein, E. and Kopelman, I.J. (1985) Convective heating rate parameters of model solutions in an agitating retort simulator. Lebensmittel-Wissenschaft und Technologie 18, 311-315.

Knap, R.P. and Durance, T.D. (1998). Thermal processing of suspended food particles in cans with end-over-end agitation. Food Research International 31 (9), 635-643.

Naveh, D. and Kopelman, I.J. (1980). Effect of some processing parameters on the heating transfer coefficients in a rotating autoclave. Journal of Food Processing and Preservation 4, 67-77.

Parchomchuk, P. (1977). A simplified method for agitation processing of canned foods. Journal of Food Science 42, 265-268.

Ramaswamy, H.S., Abbatemarco, C. and Sablani, S.S. (1993). Heat transfer rates in a canned food model as influenced by processing in an end over end rotary steam/air retort. Journal of Food Processing and Preservation 17, 269- 286.

Rao, M.A. and Anantheswaran, R.C. (1988). Convective heat transfer to fluid foods in cans. Advances in Food Research 32, 38-84. Academic Press, Inc. London, UK.

Sablani, S.S. and Ramaswamy, H.S. (1995). Fluid to particle heat transfer coefficients in cans during end over end processing. Lebensmittel-Wissenschaft und Technologie 28, 56-61.

Stoforos, N.G., and Merson, R.L. (1991). Measurement of heat transfer coefficients in rotating liquid/particulate systems. Biotechnology Progress 7, 267-271.

Stoforos, N.G. and Merson, R.L. (1992). Physical property and rotational speed effects on heat transfer in axially rotating liquid/particulate canned foods. Journal of Food Science 57, 749-754.

Tucker, G.S., Noronna, J.F. and Heydon, C.J. (1996). Experimental validation of mathematical procedures for the evaluation of thermal processes and process deviations during the sterilisation of canned foods. Transactions of the Institute of Chemical Engineers 74, Part C, 140-147.

APPENDIX 1

Rheological data for tomato sauce at elevated temperatures

Rheogram for tomato sauce at 40°C to calculate the consistency co-efficient (k) and the flow behavour index (n)

Up curve

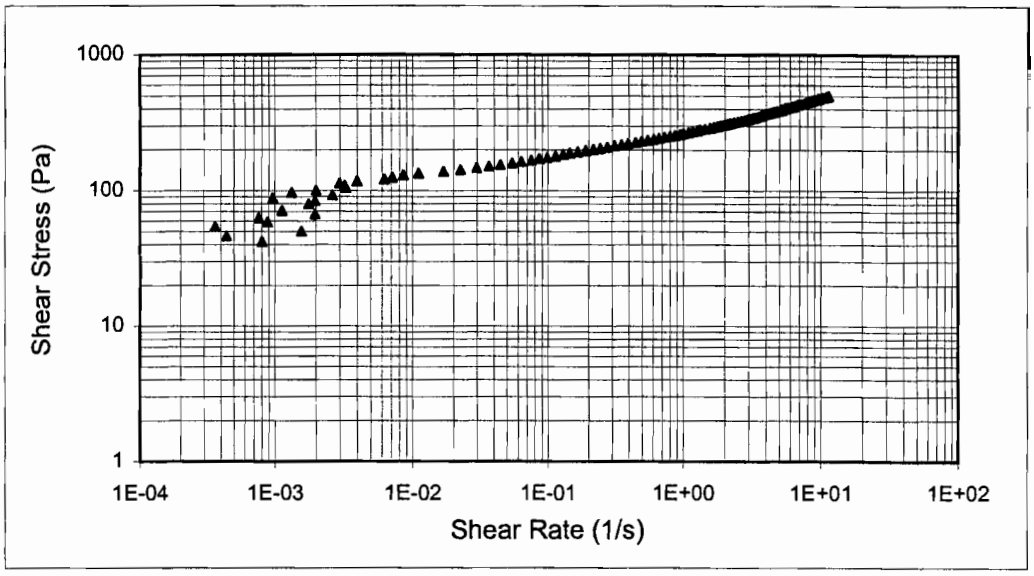

Down curve

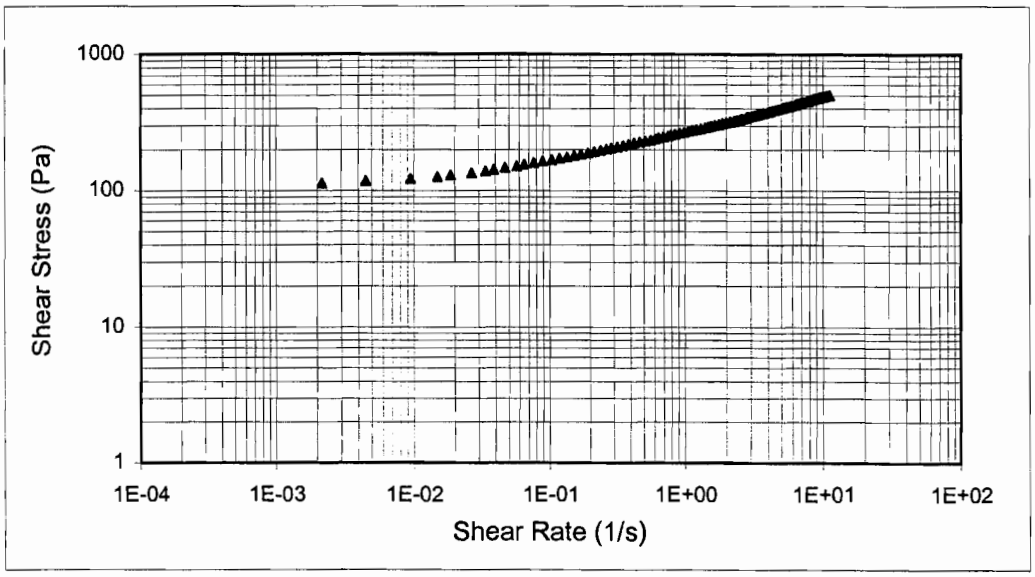

Up	**k:**	**25.55845 Pa.sn**	**Down**	**k:**	**26.37192 Pa.sn**
	n:	**0.269957**		**n:**	**0.263302**

Rheogram for tomato sauce at 50°C to calculate the consistency co-efficient (k) and the flow behavour index (n)

Up curve

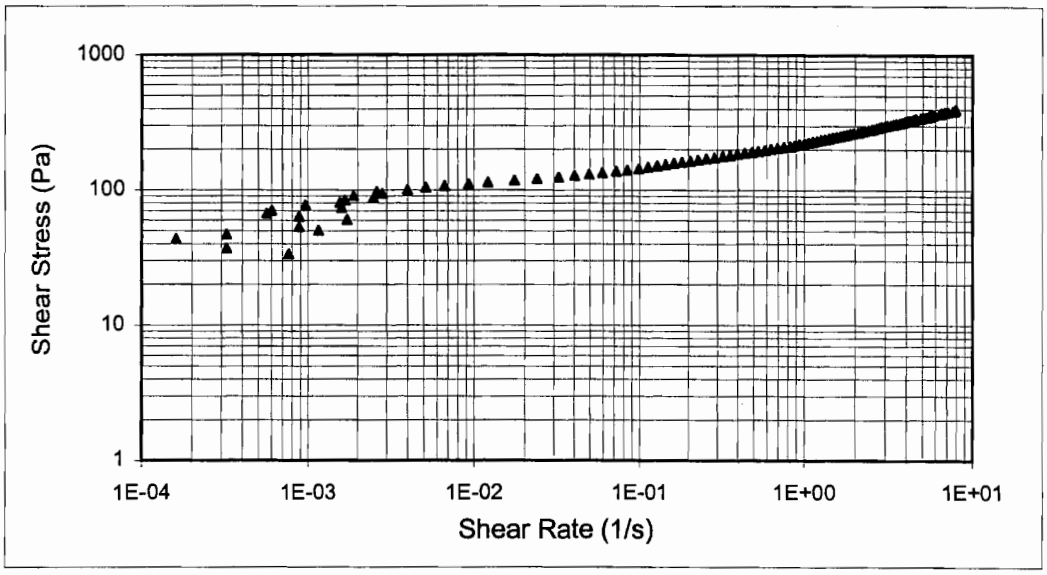

Down curve

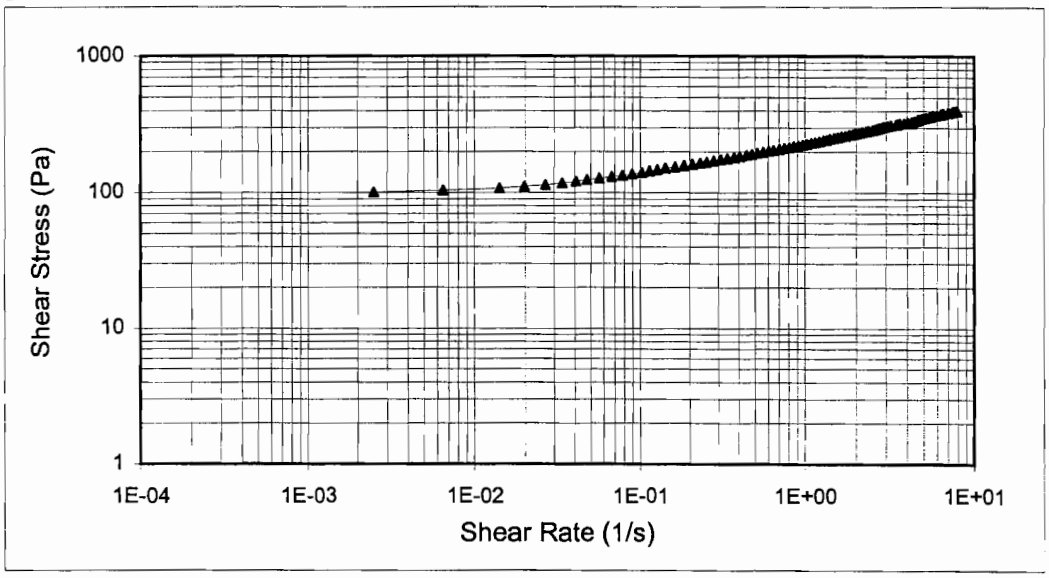

Up	**k:**	**21.94406 Pa.sn**	**Down**	**k:**	**22.56021 Pa.sn**
	n:	**0.28342**		**n:**	**0.277454**

Rheogram for tomato sauce at 60°C to calculate the consistency co-efficient (k) and the flow behavour index (n)

Up curve

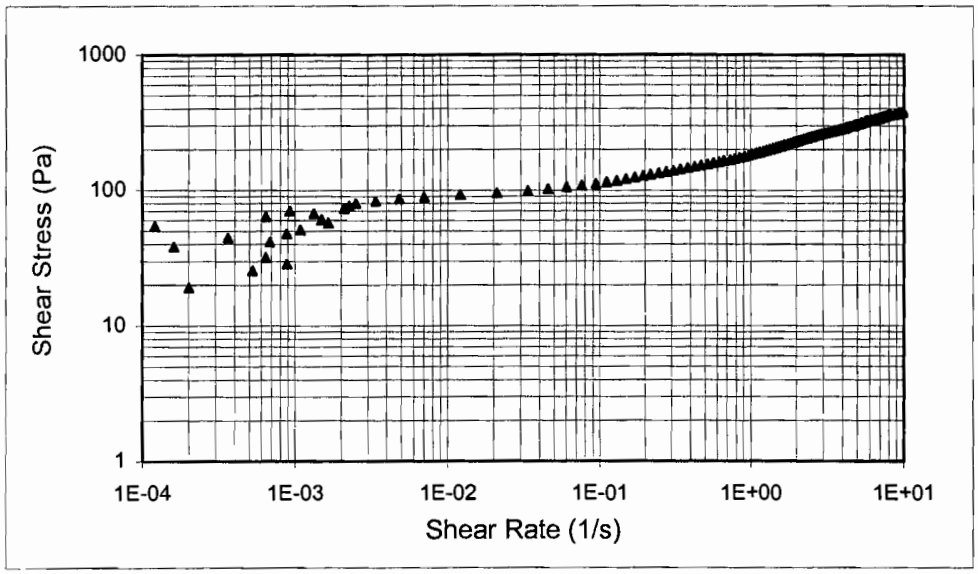

Down curve

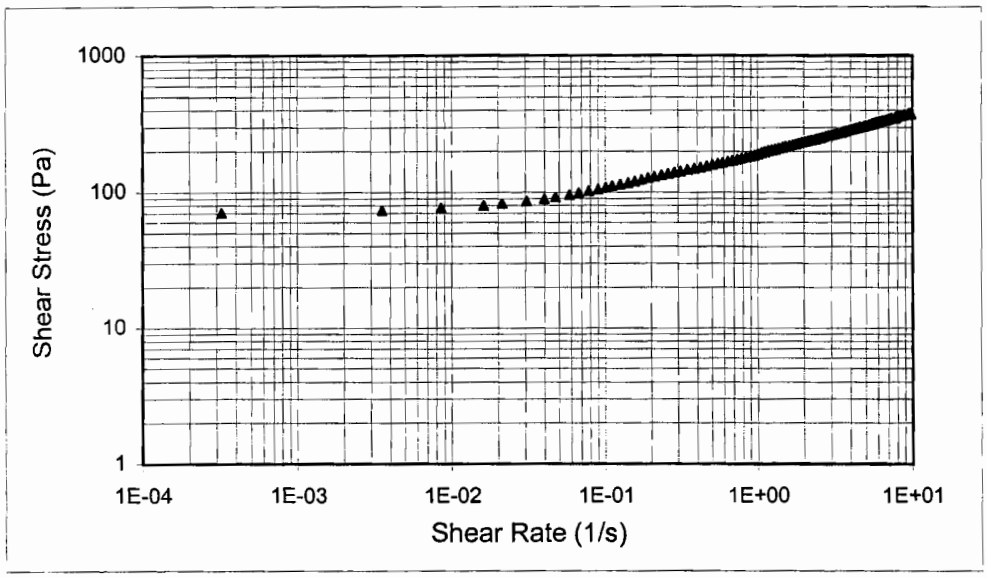

Up	k:	18.46 Pa.s^n	Down	k:	19.08 Pa.s^n
	n:	0.32		n:	0.3

Rheogram for tomato sauce at 70°C to calculate the consistency co-efficient (k) and the flow behaviour index (n)

Up curve

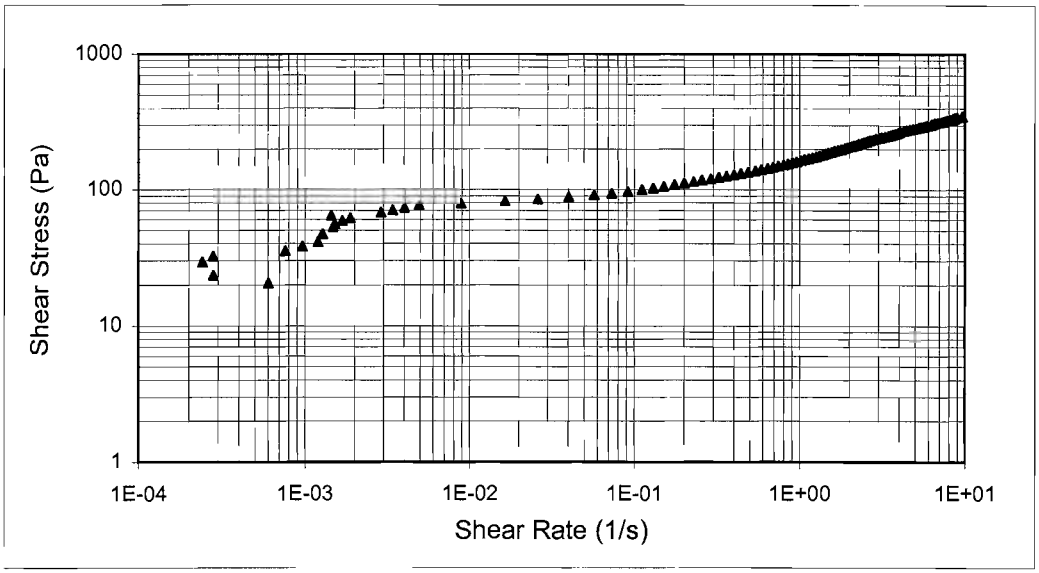

Down curve

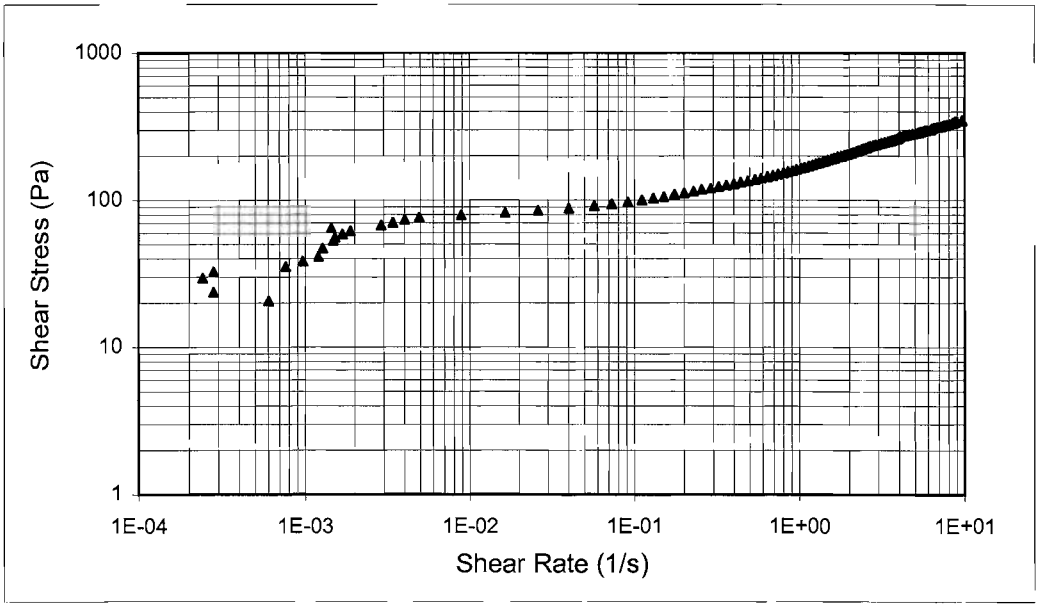

Up	**k:**	**16.47018 Pa.sn**	**Down**	**k:**	**17.29425 Pa.sn**
	n:	**0.336362**		**n:**	**0.313475**

Rheogram for tomato sauce at 80°C to calculate the consistency co-efficient (k) and the flow behavour index (n)

Up curve

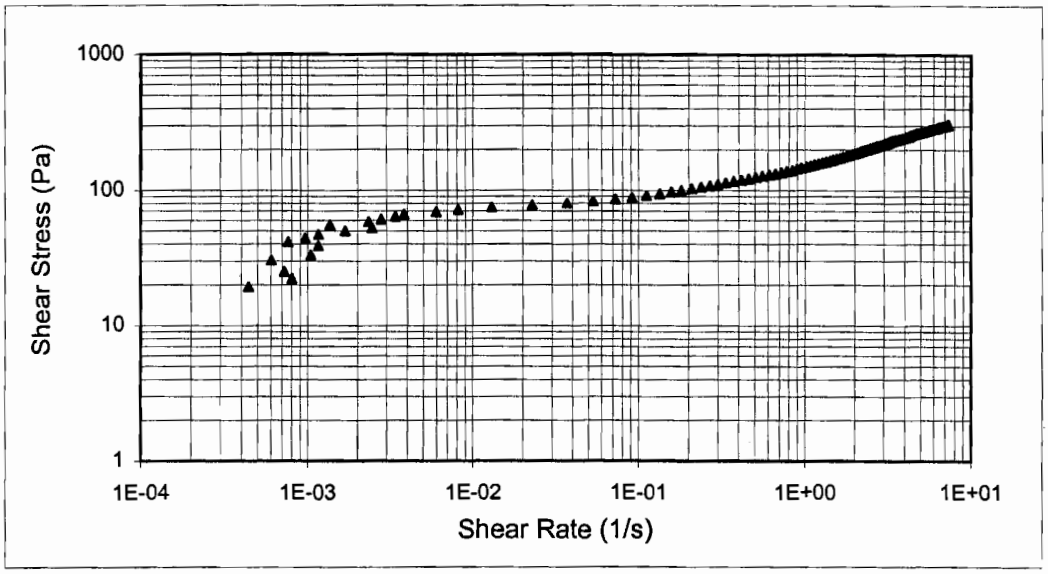

Down curve

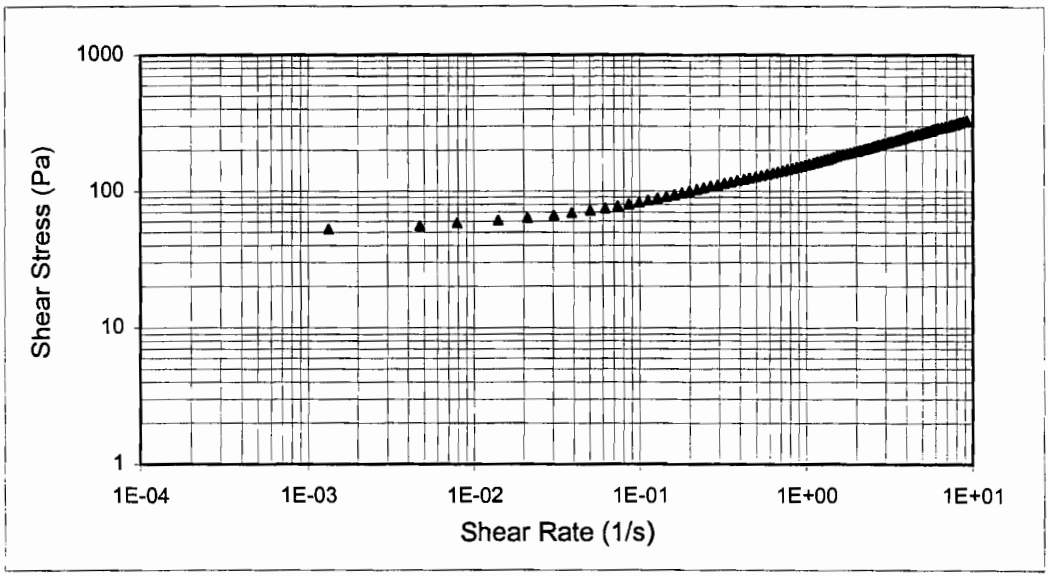

Up	**k:**	**14.62393 Pa.sn**	**Down**	**k:**	**15.56614 Pa.sn**
	n:	**0.372025**		**n:**	**0.337958**

APPENDIX 2

Rheological data for Colflo 67 at ambient temperature

Rheogram for 5.5% Colflo 67 solution at 25°C

Up curve

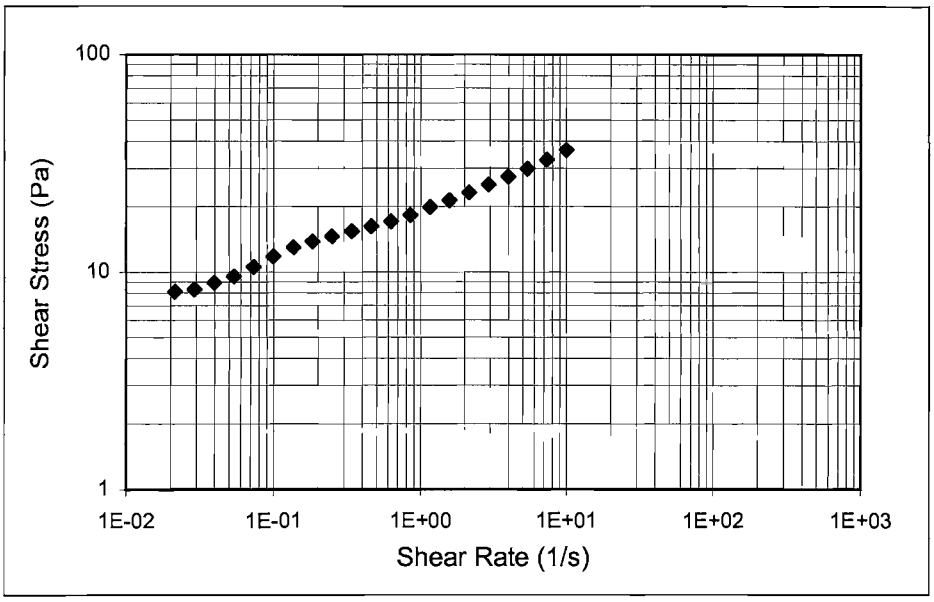

Down curve

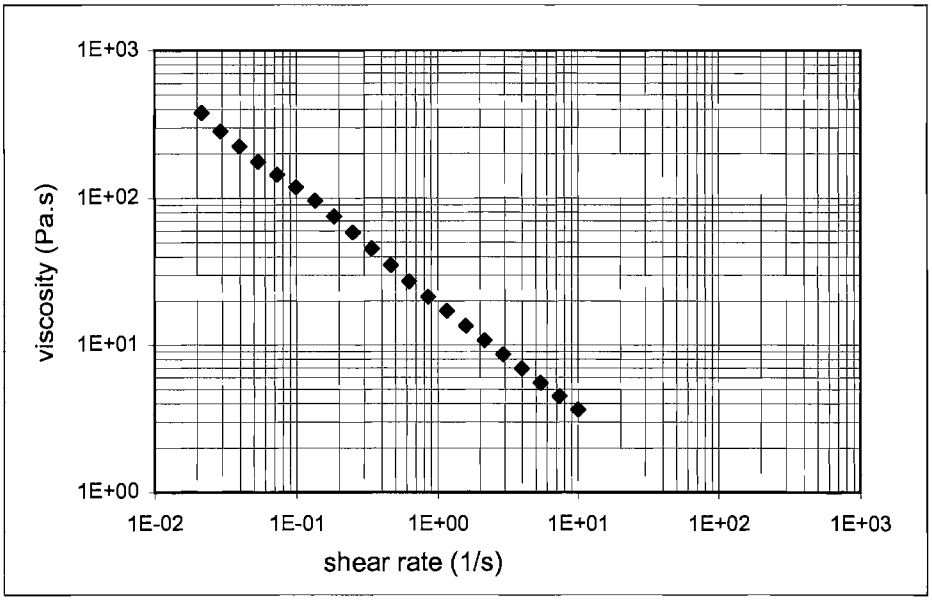

Flow behaviour index (95% CIs)

n = 0.24
n_{min} = 0.22
n_{max} = 0.25

General consistency coefficient (95% CIs)

k = 19.84 $Pa.s^n$
k_{min} = 19.44 $Pa.s^n$
k_{max} = 20.25 $Pa.s$

Rheogram for 6.0% Colflo 67 solution at 25°C

Up curve

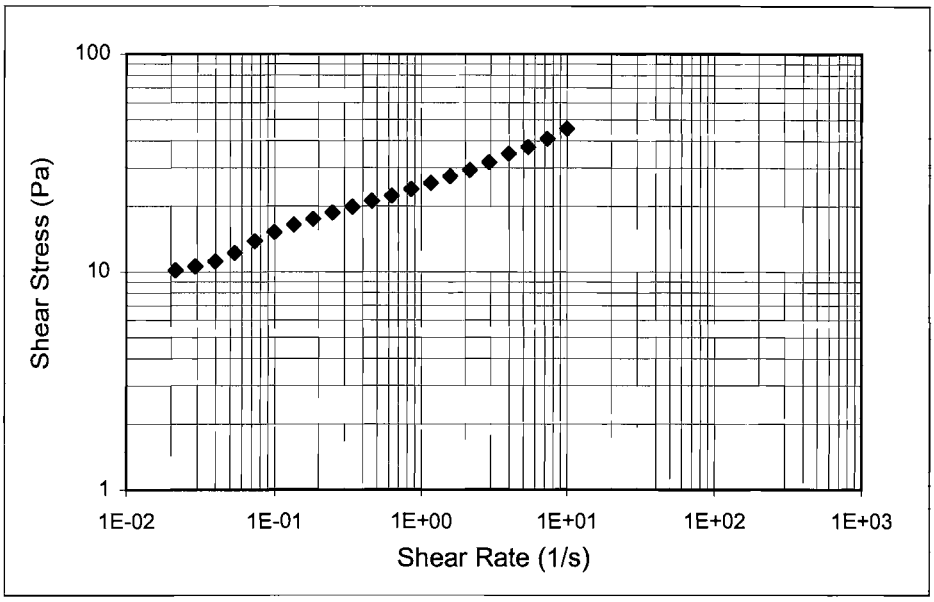

Down curve

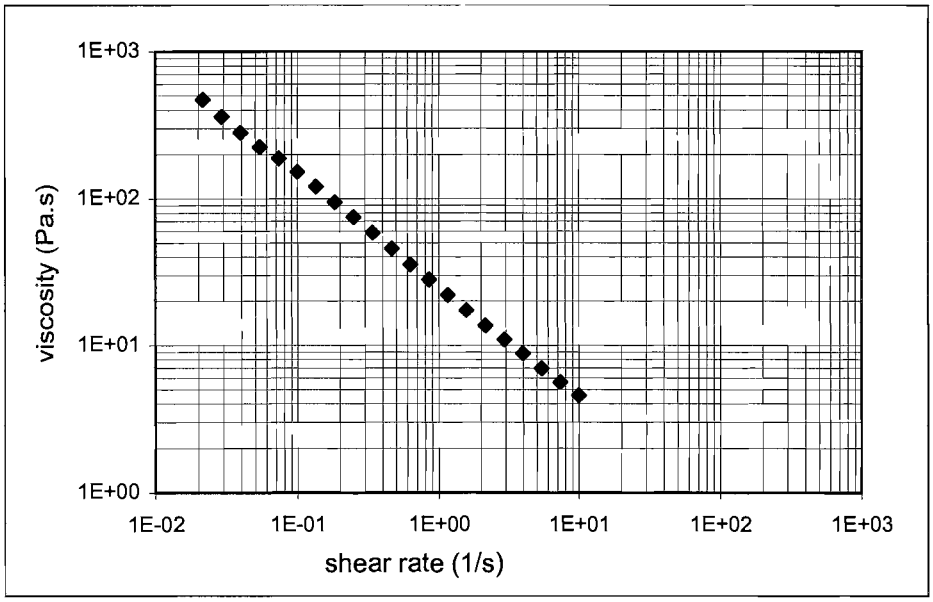

Flow behaviour index (95% CIs)

n = 0.23
n_{min} = 0.22
n_{max} = 0.24

General consistency coefficient (95% CIs)

k = 25.35 $Pa.s^n$
k_{min} = 24.99 $Pa.s^n$
k_{max} = 25.71 $Pa.s$

Rheogram for 6.5% Colfo 67 solution at 25°C

Up curve

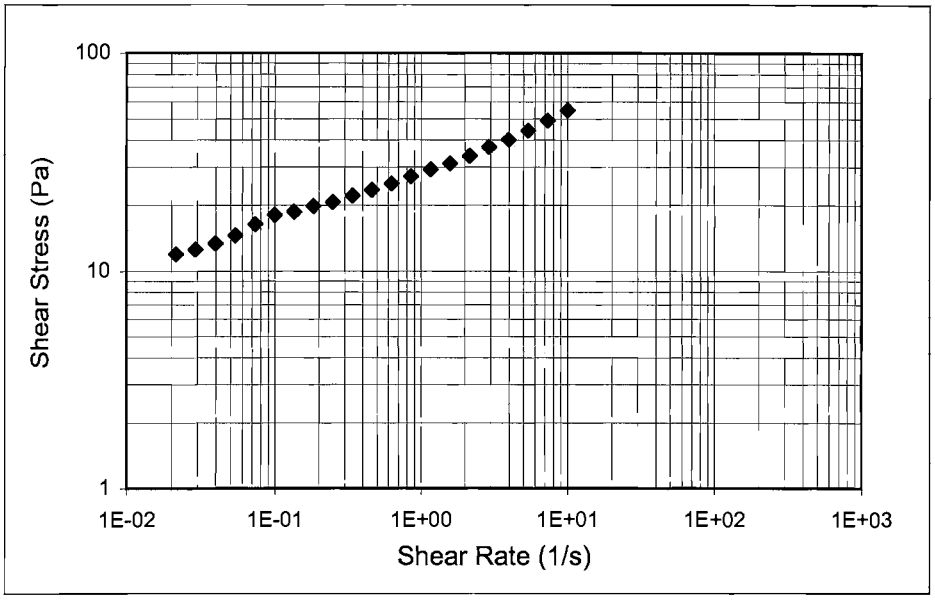

Down curve

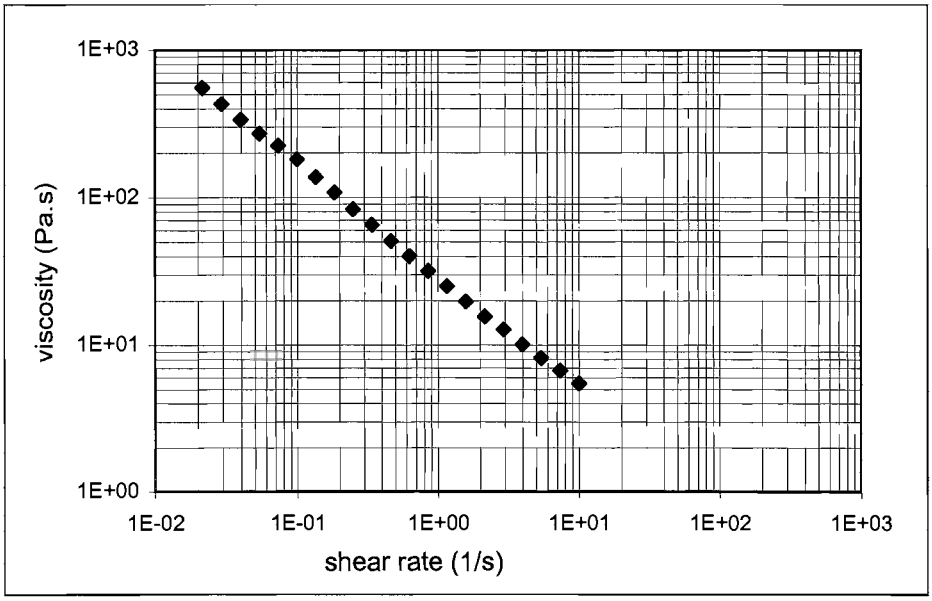

Flow behaviour index (95% CIs)

n = 0.25
n_{min} = 0.23
n_{max} = 0.26

General consistency coefficient (95% CIs)

k = 29.01 $Pa.s^n$
k_{min} = 28.43 $Pa.s^n$
k_{max} = 29.59 $Pa.s$

Rheogram for 7.0% Colflo 67 solution at 25°C

Up curve

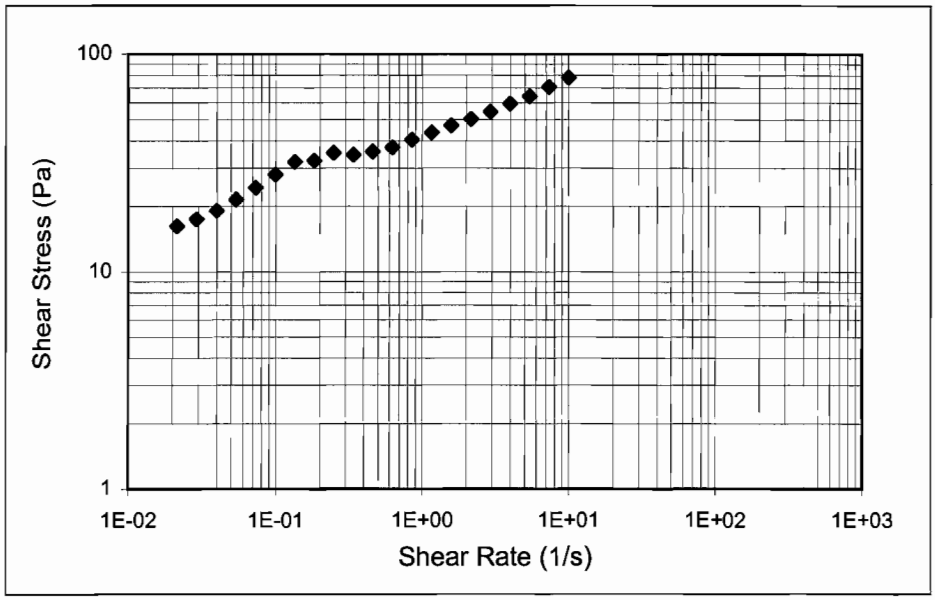

Down curve

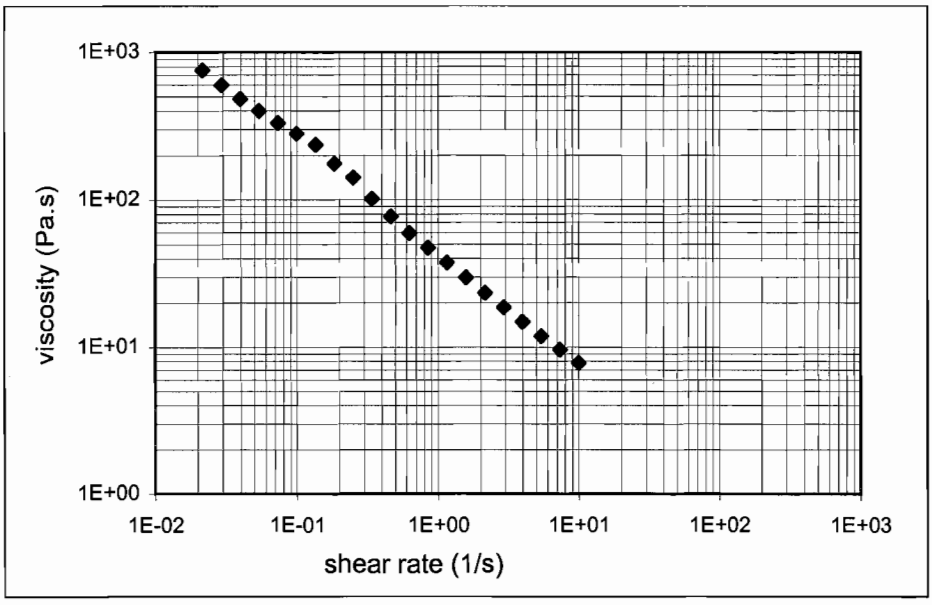

Flow behaviour index (95% CIs)

n = 0.21
n_{min} = 0.19
n_{max} = 0.23

General consistency coefficient (95% CIs)

k = 44.38 $Pa.s^n$
k_{min} = 43.00 $Pa.s^n$
k_{max} = 45.80 $Pa.s$

To compare tomato sauce at elevated temperatures against Colflo 67 at ambient temperature (Colfo 67 at 7.0, 6.5, 6.0 and 5.5 %; tomato sauce at 40, 50, 60, 70 and 80°C)

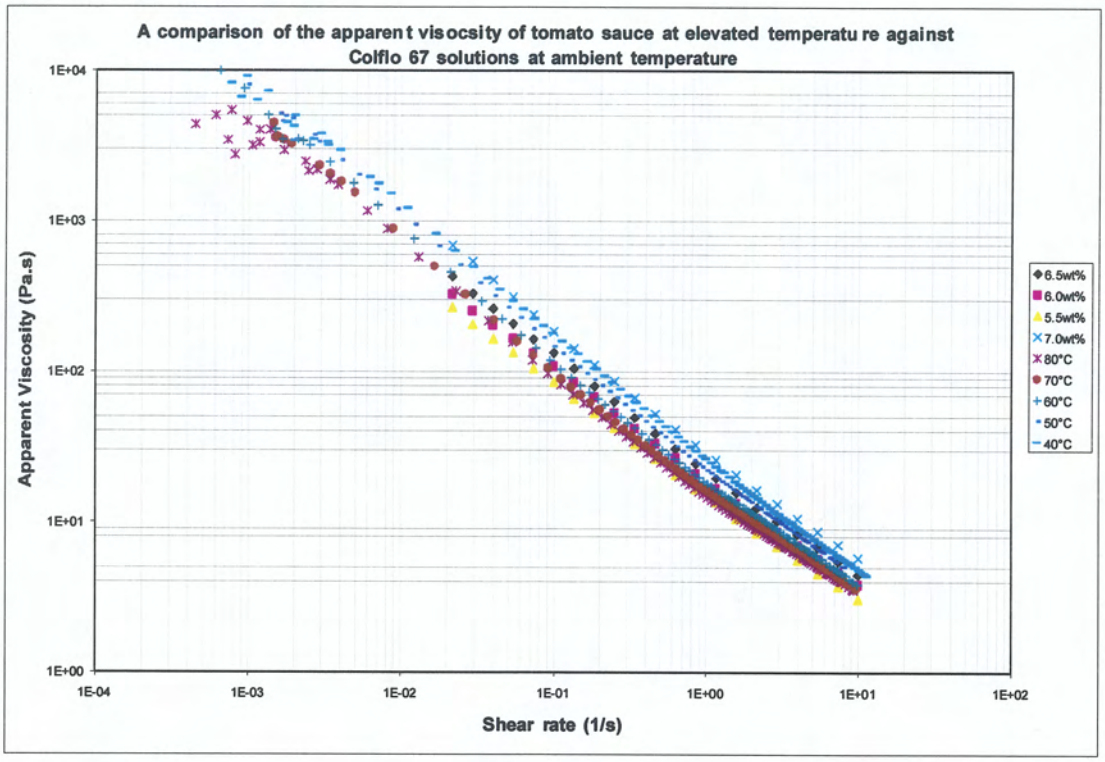

APPENDIX 3

Flow visualisation results for Colflo 67 solutions matching tomato sauce at elevated temperatures showing the amount of mixing by the incorporation of blue dye into the solutions

5.48% Starch

Time elapsed

1 minute

2 minutes

3 minutes

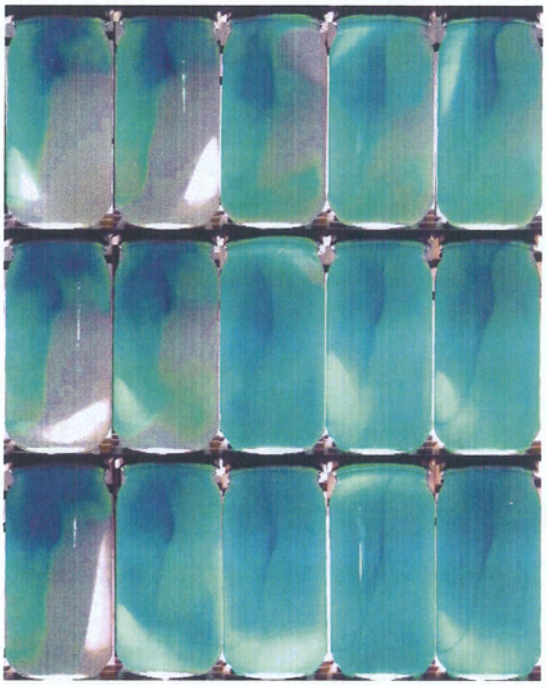

Rotation speed 15 20 25 27 30
RPM

5.58% Starch

Time elapsed

1 minute

2 minutes

3 minutes

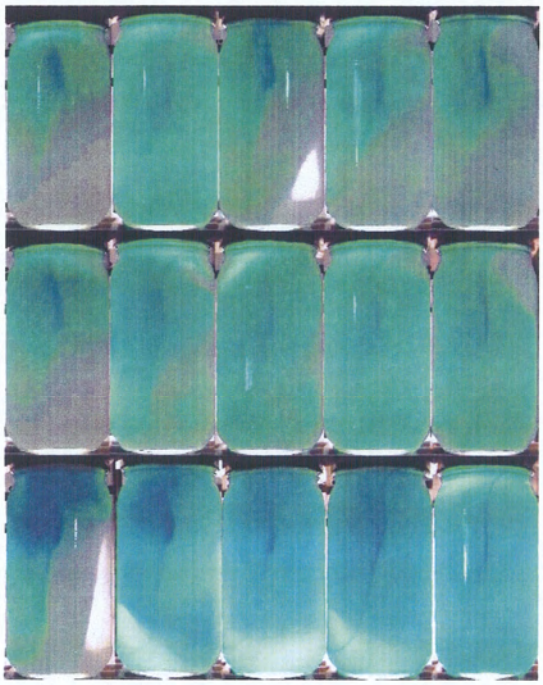

Rotation speed 15 20 25 27 30
RPM

Starch 5.73%

Time elapsed

1 minute

2 minutes

3 minutes

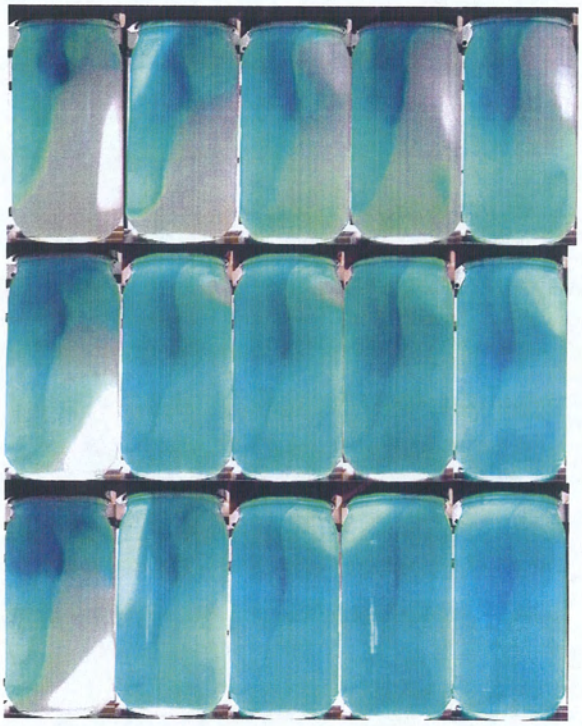

Rotation speed 15 20 22 25 30

RPM

Starch 5.97%

Time elapsed

1 minute

2 minutes

3 minutes

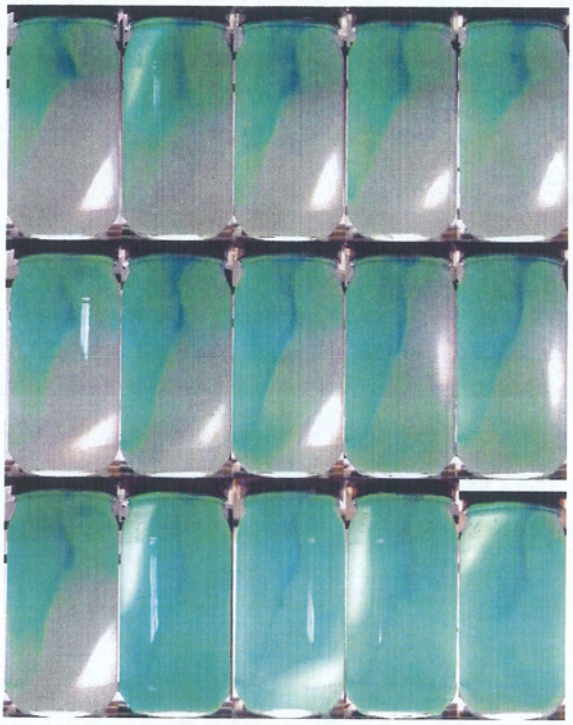

Rotation speed

15 20 22 25 30

RPM

Starch 6.29%

Time elapsed

1 minute

2 minutes

3 minutes

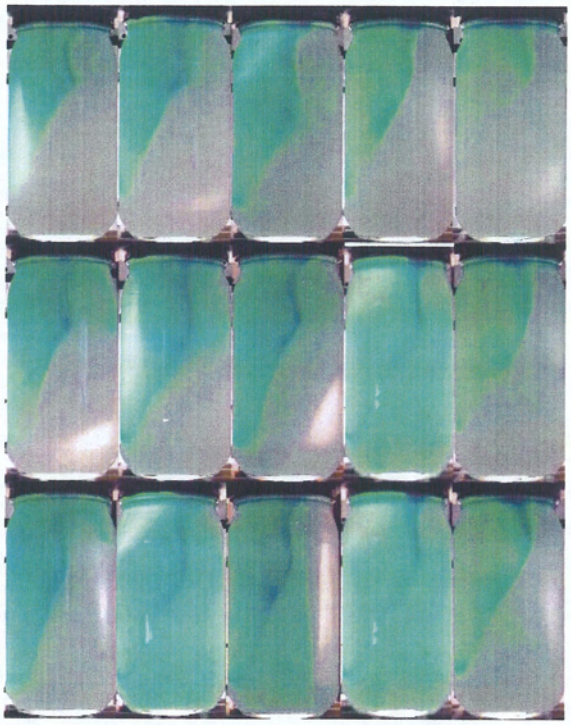

Rotation speed 15 20 22 25 30

APPENDIX 4

Predicted processing profiles for factory trials under normal, manually interrupted and automatically timed processes

Manual interuption T/C 2

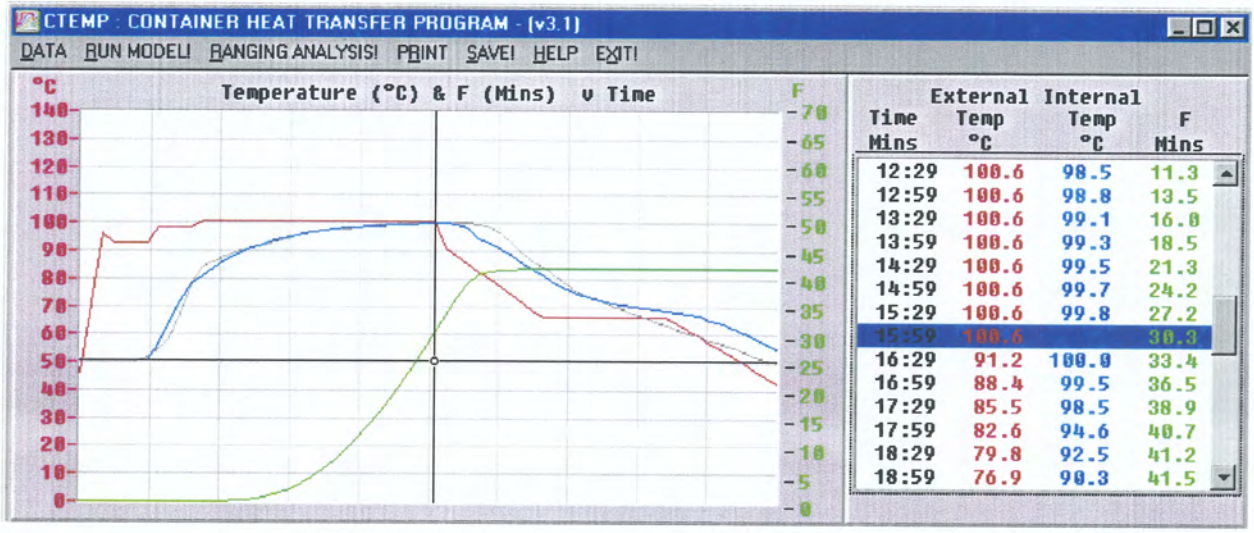

Environmental temperature
Predicted profile
Product profile
Cumulative P value

Manual interuption T/C 3

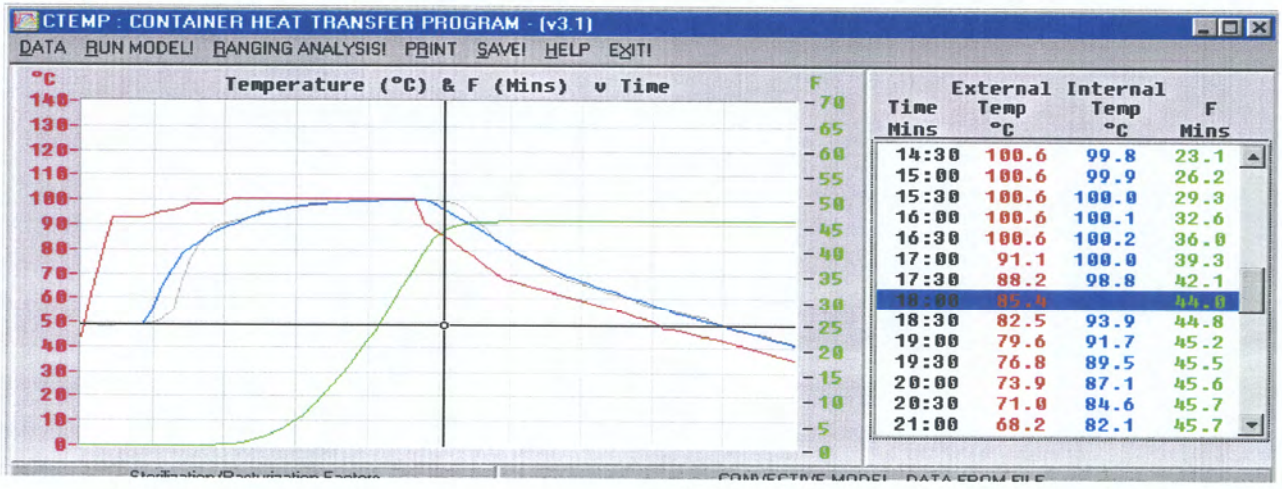

Manual interuption T/C4

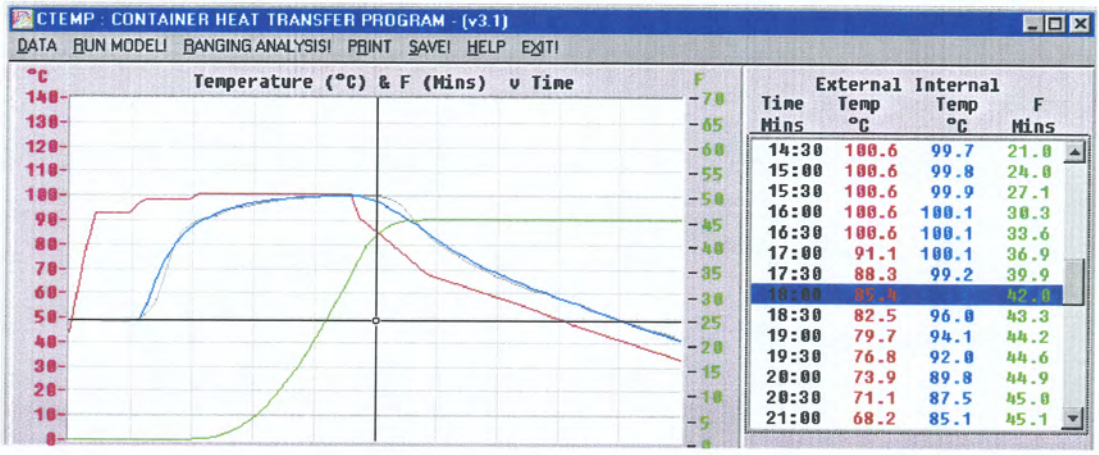

Environmental temperature
Predicted profile
Product profile
Cumulative P value

Automatic timed T/C 2

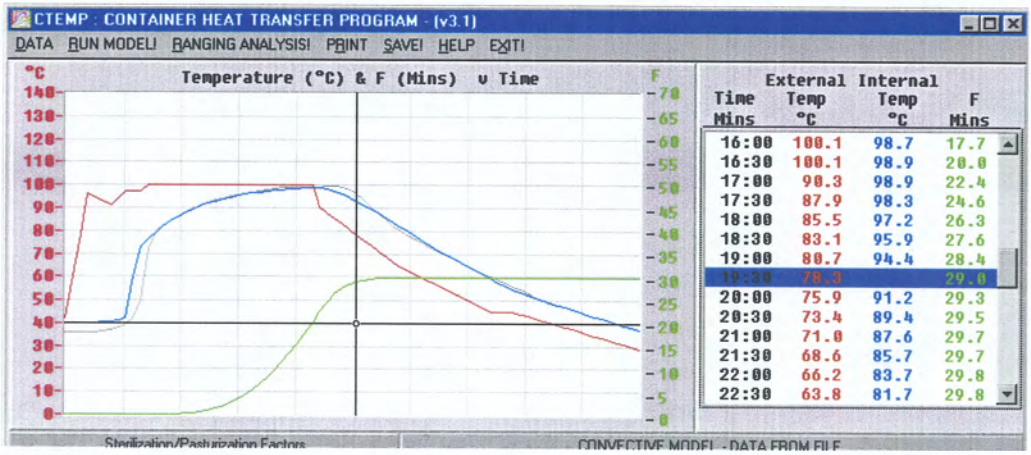

Automatic timed T/C 3

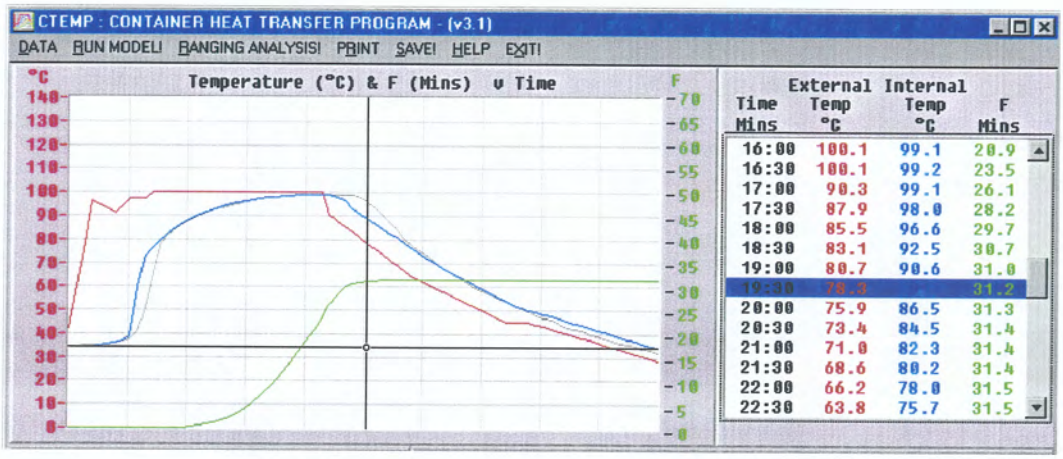

Environmental temperature
Predicted profile
Product profile
Cumulative P value

Automatic timed T/C 4

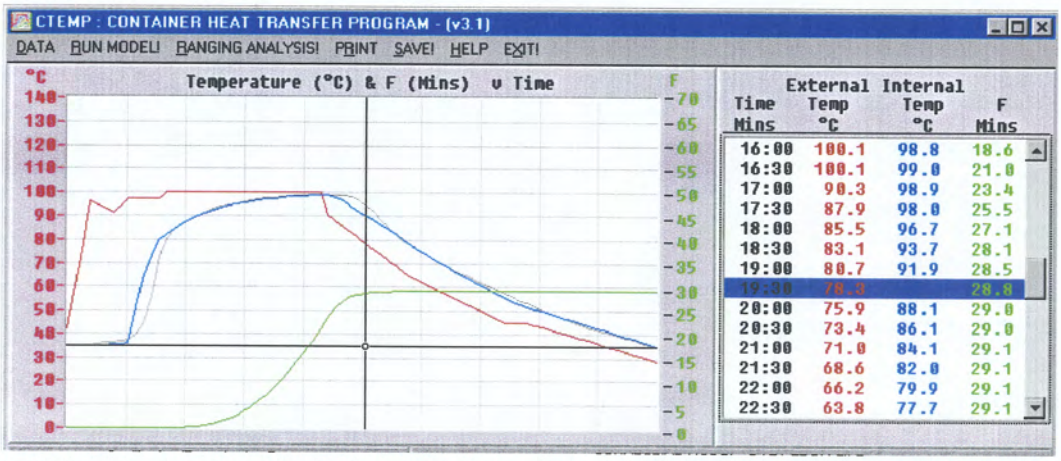

Standard process T/C 2

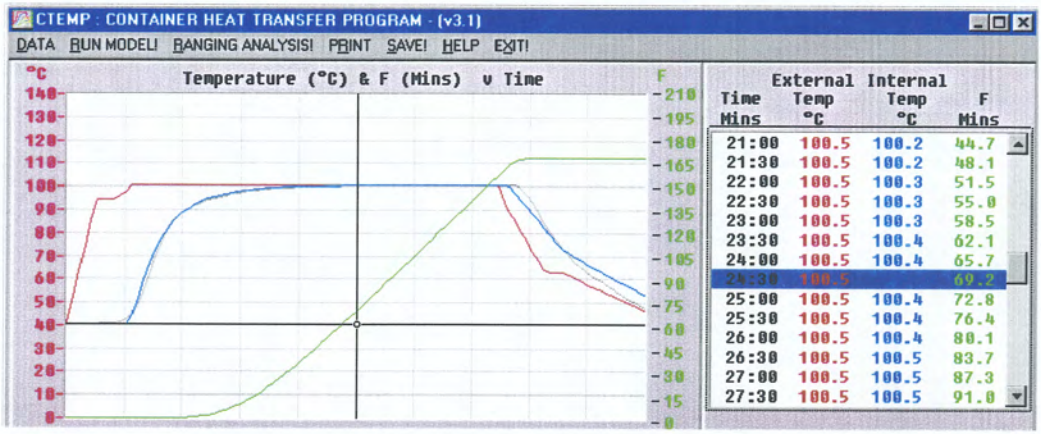

Environmental temperature
Predicted profile
Product profile
Cumulative P value

Standard process T/C 3

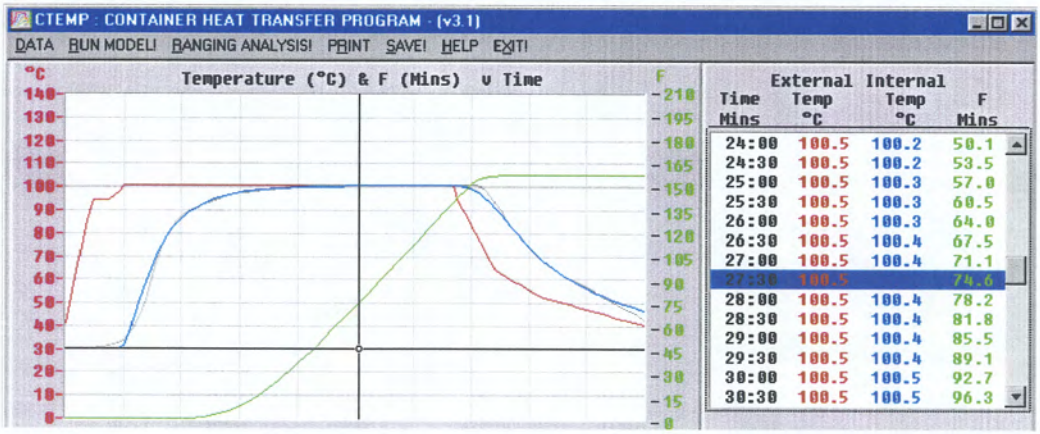

Standard process T/C 4

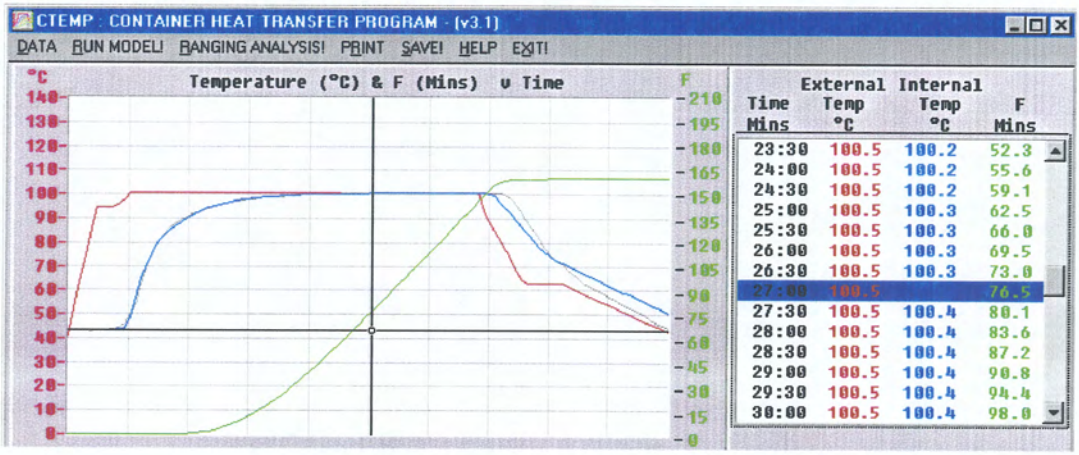

Environmental temperature
Predicted profile
Product profile
Cumulative P value

APPENDIX 5

Heating profiles for factory trials

Figure 1: Heating profile for manually interrupted process

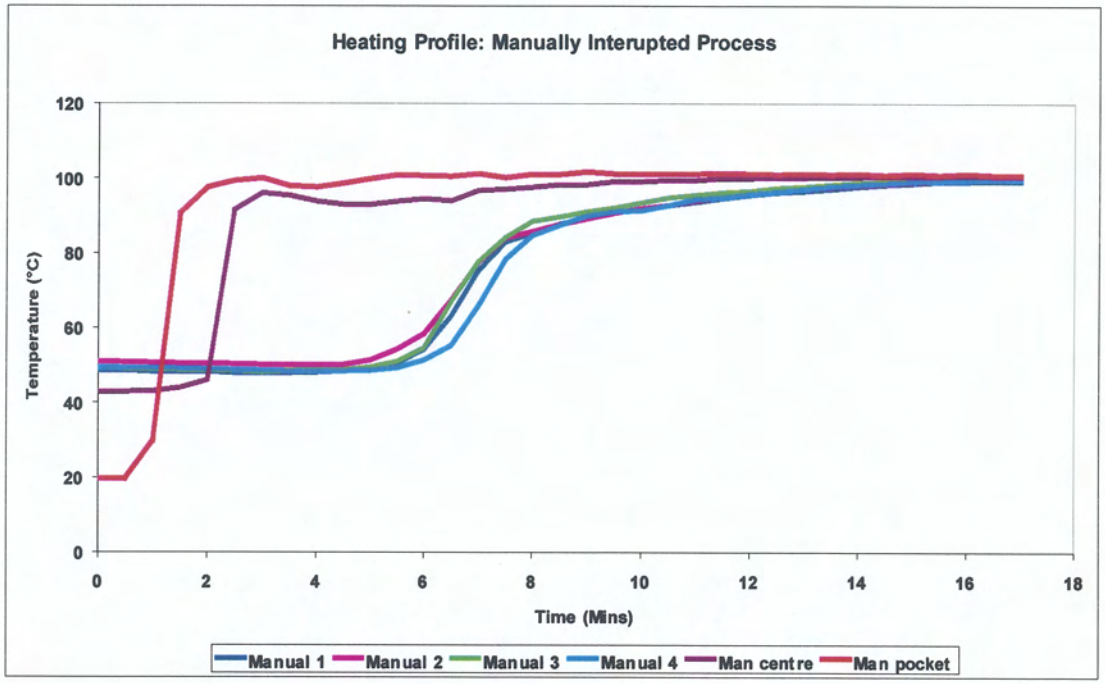

Figure 2: Heating profile for automatically timed process

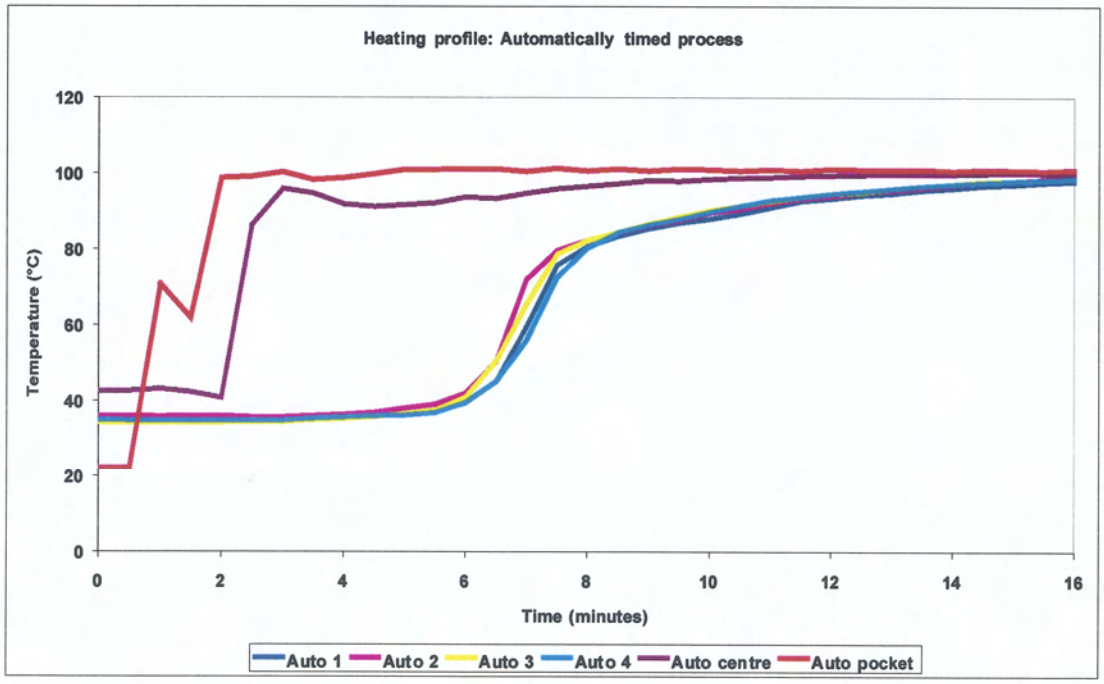

Figure 3: Heating profile for standard processing conditions